Theory of correlations in stochastic neural networks

Iris Ginzburg

*School of Physics and Astronomy, Beverly and Raymond Sackler Faculty of Exact Sciences, Tel-Aviv University,
Tel-Aviv 69978, Israel*

Haim Sompolinsky

*Racah Institute of Physics and Center for Neural Computation, Hebrew University, Jerusalem 91904, Israel
and AT&T Bell Laboratories, Murray Hill, New Jersey 07974*

One of the main experimental tools in probing the interactions between neurons has been the measurement of the correlations in their activity. In general, however the interpretation of the observed correlations is difficult since the correlation between a pair of neurons is influenced not only by the direct interaction between them but also by the dynamic state of the entire network to which they belong. Thus a comparison between the observed correlations and the predictions from specific model networks is needed. In this paper we develop a theory of neuronal correlation functions in large networks comprising several highly connected subpopulations and obeying stochastic dynamic rules. When the networks are in asynchronous states, the cross correlations are relatively weak, i.e., their amplitude relative to that of the autocorrelations is of order of $1/N$, N being the size of the interacting populations. Using the weakness of the cross correlations, general equations that express the matrix of cross correlations in terms of the mean neuronal activities and the *effective interaction matrix* are presented. The effective interactions are the synaptic efficacies multiplied by the gain of the postsynaptic neurons. The time-delayed cross-correlation matrix can be expressed as a sum of exponentially decaying modes that correspond to the (nonorthogonal) eigenvectors of the effective interaction matrix. The theory is extended to networks with random connectivity, such as randomly dilute networks. This allows for a comparison between the contribution from the internal common input and that from the direct interactions to the correlations of monosynaptically coupled pairs. A closely related quantity is the linear response of the neurons to external time-dependent perturbations. We derive the form of the dynamic linear response function of neurons in the above architecture in terms of the eigenmodes of the effective interaction matrix. The behavior of the correlations and the linear response when the system is near a bifurcation point is analyzed. Near a saddle-node bifurcation, the correlation matrix is dominated by a single slowly decaying critical mode. Near a Hopf bifurcation the correlations exhibit weakly damped sinusoidal oscillations. The general theory is applied to the case of a randomly dilute network consisting of excitatory and inhibitory subpopulations, using parameters that mimic the local circuit of 1 mm^3 of the rat neocortex. Both the effect of dilution as well as the influence of a nearby bifurcation to an oscillatory state are demonstrated.

PACS number(s): 87.10.+e

I. INTRODUCTION

Cross-correlation (CC) measurements are among the major experimental tools for studying the synaptic interactions between neurons. For a review of the experimental methods and results see Refs. [1,2]. Time-delayed CCs between proximal neurons often exhibit a pronounced delay and are usually interpreted as resulting from a direct interaction between the correlated pair. The majority of CCs between distal neurons in cortex exhibit a "central peak." This has been taken as an indication of the presence of a "common input" to both neurons, which synchronizes their activity. The origin of this input is in general not known. While in some cases it may originate from other brain areas, it is reasonable to expect that synaptic currents from the local circuits to which the two correlated neurons belong contribute significantly to their correlations. Thus the correlations may be an im-

portant tool in studying the cooperative dynamics of the local circuits in the cortex and other neuronal systems.

Neuronal correlations serve as a convenient measure of the temporal synchrony of the activities of neurons. This synchrony may have important implications on the function of the network. First, it affects the utility of using population codes to overcome the noise in the neural responses to external stimuli [3,4]. Moreover, the synchrony may be utilized to encode or transmit information, as suggested by recent studies of spatiotemporal patterns of neuronal responses in olfactory [5,6], visual [7–10], and association areas [2,11] in cortex. Final, understanding of the correlations in neuronal activity is important for uncovering some of the mechanisms underlying plasticity and learning [12]. Unfortunately, very little is known theoretically about the properties of CCs in large networks. Hence the interpretation of the observed features of the CCs remains an open challenge and is the topic of this paper.

<u>50</u>   3171

Another potentially important probe of the interactions in a neuronal network is the linear response function, namely, the change in the average firing rates due to a sufficiently weak externally applied perturbation. Here again, the magnitude as well as the temporal evolution of the response depend on the state of the network. Hence it is important to understand the properties of linear response functions in large networks.

Most of the theoretical studies of neural network models consider only average firing rates, where the averaging is over time, over the stochastic noise, or over a population of neurons. In many highly connected networks these averages obey relatively simple mean-field equations. However, to account for the fluctuations about these averages, one must go beyond the mean-field equations. In this work we develop the theory of the fluctuations in the neuronal activities and their correlations in large stochastic networks. We focus on network architectures that allow a mean-field description of their average activities. Specifically, we assume that the network comprises several large, homogeneous subpopulations, each consists of a significant fraction of the total number of neurons N. Each neuron is coupled to order N neighbors; hence the individual synaptic efficacies are weak, i.e., of order $1/N$. Other important restrictions of the present work are concerned with the dynamics. We assume that the network obeys stochastic dynamic equations and that it is in an asynchronous state. Under the above conditions we derive equations for the dynamic linear response and time-dependent correlation functions. These expressions reveal the relationship between the correlations and the linear response functions on one hand and the network connectivity and dynamical state on the other. These results are extended to the case of networks with randomness in the connections. We apply the general theory to a network composed of two subpopulations: excitatory neurons and inhibitory ones. We calculate the time-delayed autocorrelation (AC) and CC functions using parameters that represent the gross features of the local connectivity and the rest activity levels in the rat neocortex. The effect of a proximity of a bifurcation to a synchronized oscillatory state as well as the effect of random dilution of the connections are elucidated.

The outline of the paper is as follows. In Sec. II we define asynchronous and synchronous states in large neural networks and discuss their implications. In Sec. III, we define the stochastic dynamics of the networks, describe the neuronal correlation functions, and present some of their general properties. We then define the mean-field architecture which will be assumed in most of this work. The mean-field equations for the noise- or population-averaged activities are derived in Sec. IV. In Sec. V we derive the linear response of the average activities to a small change in the external stimulus. In Sec. VI explicit equations for the equal-time and time-delayed correlations in these networks are derived. We also discuss briefly the decomposition of an observed CC matrix. The critical behavior of correlations and linear response near a bifurcation point is discussed in Sec. VII. Section VIII extends the theory to include random connections. In Sec. IX we

apply the general theory to a randomly diluted network composed of excitatory and inhibitory populations. The results of the paper are discussed in Sec. X. Preliminary results of part of the work have been reported in Ref. [13].

II. ASYNCHRONOUS STATES IN LARGE NETWORKS

In most of the interesting neural networks, the degree of connectivity is such that the overwhelming majority of the neurons are interacting at least indirectly and the temporal fluctuations in their activity will always be at least partially correlated. Nevertheless, in large networks there is a clear distinction between synchronous and asynchronous dynamic states, according to the degree of synchrony in the network. To make this distinction precise, one has to consider the behavior of the correlations as a function of the size of the network. *In a synchronous state*, the CCs between a finite fraction of the neurons in the network remain finite even in the limit of $N \to \infty$, N being the size of the network. *In an asynchronous state*, the CCs between most of the pairs vanish in the limit of large N. Note that the CCs are defined so that they vanish for a pair of random uncorrelated variables; see Eq. (3.5) below.

The amplitude of the CCs, in the asynchronous state, depends on the pattern of connectivity. In networks with short-range interactions the CCs between neighboring pairs will be typically of order 1 even for large N. However, the magnitude of the CCs will fall off with the distance between the pair. In the most common cases this fall off has a characteristic microscopic length ξ, beyond which the correlations decay exponentially as

$$C(R_{ij}) \propto \exp(-R_{ij}/\xi) \ . \quad R_{ij} \gg \xi \ . \qquad (2.1)$$

where R_{ij} is the distance between the neurons i and j. The correlation length is much smaller than the linear size of the system L, implying that the CCs between most of the pairs, which are separated by order L, are exponentially small in L. In certain stochastic models, the generic falloff of $C(R)$ is only algebraic in R^{-1}. Even in these cases, the CCs between neurons separated by $R \approx L$ are vanishingly small as $L \to \infty$.

In this work we consider highly connected networks, meaning that each neuron is connected directly to a finite fraction of all the neurons in the network. In this case, the connections are weak, typically of order $1/N$. Otherwise, the total synaptic input to a neuron will drive it well into saturation. The asynchronous states in such networks are characterized by CCs which are not exponentially small but still vanish for large N. The generic scaling is

$$C \propto \frac{1}{N} \ , \quad N \to \infty \ . \qquad (2.2)$$

Note that even in the asynchronous state, the CCs have significant or even dominant contributions from indirect pathways between pairs. Still the scaling of all these contributions with N is the same as that of the direct

connections. There are special circumstances in which the correlations are larger than that of Eq. (2.2), even in asynchronous states. An example is the case where there is a precise balance between positive and negative connections in the networks. Such is the case in infinite-range spin glasses [14] or in the Hopfield model of associative memory near saturation [15]. In these cases, the connections and the CCs scale as

$$C \propto \frac{1}{\sqrt{N}} \quad , \quad N \to \infty \ . \tag{2.3}$$

However, the mean-field theory of these networks, even for the average activities, is complicated and is outside the scope of the present work.

As stated above, synchronous states are characterized by CCs that remain of order 1 even in the limit of large N. These strong correlations reflect the appearance of globally synchronized temporal patterns. Note that the same system can switch from an asynchronous state to a synchronous one by changing the value of one of its parameters. Synchronous states can appear in both short-range and long-range systems. However, in large short-range systems, stable synchronous states are in most cases periodic or quasiperiodic; stable chaotic synchronized states are rare [16,17]. On the other hand, systems with long-range interactions can have periodic or chaotic synchronous states. The nature of the correlations in synchronous states in fully connected networks is discussed elsewhere [18].

The above characterization of asynchronous states is difficult to check in experimental systems since it requires reliable estimates of such parameters as the size of the network and the strength of connections. An alternative characterization is based on the behavior of population averages. Let us denote by $x_i(t)$ a local observable, e.g., the instantaneous rate of the ith neuron. Let us suppose that we can measure the mean of this quantity over a subpopulation of size K, where $K \ll N$, yielding

$$X_K(t) \equiv \frac{1}{K} \sum_i^K x_i(t) \ . \tag{2.4}$$

Asynchronous states can be distinguished from synchronous states according to the K dependence of the variance of X,

$$\Delta(K) \equiv \langle [X_K(t) - \langle X_K \rangle]^2 \rangle \ , \tag{2.5}$$

where $\langle \ \rangle$ denotes averaging over time. In asynchronous states the local variables are weakly correlated; hence

$$\Delta(K) \propto \frac{1}{K}, \quad 1 \ll K \ . \tag{2.6}$$

On the other hand, in synchronous states $\Delta(K) \sim 1$ even for large K. The advantage of this criterion is that it does not rely on the absolute scale of Δ, but on its dependence on K which, unlike N, can be varied experimentally. The limitation of this criterion is that the sampling of the x_i's and the value of K should be such that the sums are not dominated by unusually strongly correlated variables. Also, the choice of the variable x_i must be done with care

in cases where destructive interference between different types of neurons, which fluctuate out of phase from each other, is likely to occur.

III. MODEL

A. Stochastic dynamics

The network consists of N model neurons, each of which can be in one of two states, denoted by $S = 0, 1$. These states correspond to the instantaneous firing rate of the neuron, defined by short-time averaging of its spiking activity. Although the rates are in general analog variables, we assume here for simplicity that they take two discrete values: a quiescent state ($S = 0$) and a saturation rate ($S = 1$). The neurons are assumed to be exposed to local noise resulting in stochastic dynamics of their states. This dynamics is specified by transition probabilities per unit time (transition rates) between the 0 and 1 states. The transition rates are functions of the local field and the stochastic noise. The transition rates for the ith neuron takes the form

$$w(S_i \to (1 - S_i)) = \frac{1}{2\tau_0}\{1 - (2S_i - 1)[2g(h_i) - 1]\} \ , \tag{3.1}$$

where $g(h)$ is a sigmoidal function of the local field h: it is monotonically increasing, differentiable function obeying $g(-\infty) = 0$ and $g(+\infty) = 1$. The constant τ_0 is a microscopic characteristic time, presumably ranging between 5 and 10 msec. The local field acting upon the ith neuron at time t is

$$h_i(t) = \sum_{j=1}^{N} J_{ij} S_j(t) - \theta_i \ , \tag{3.2}$$

where J_{ij} denotes the synaptic efficacy between the jth presynaptic neuron and the ith postsynaptic one and θ_i represents the local threshold. Throughout the work we will assume that there is no self-coupling, i.e., $J_{ij} = 0$.

The above transition rates define a first-order Markov process [19]. It can be described by the following master equation for the probability to find the system in a state $(S_1, \ldots, S_N)$ at time t

$$\frac{d}{dt}P \ (S_1, \ldots, S_N, t)$$

$$= -\sum_{i=1}^{N} w(S_i \to (1 - S_i))P(S_1, \ldots, S_N, t)$$

$$+ \sum_{i=1}^{N} w((1 - S_i) \to S_i)$$

$$\times P(S_1, \ldots, 1 - S_i, \ldots, S_N, t) \ . \tag{3.3}$$

B. General equations for averages and correlations

Using the above master equation, a hierarchy of equations for the time evolution of moments of $\{S_i\}$ can be derived in a manner similar to that used in models with thermal equilibrium [20,21]. Here we present the equations for the first and second moments. For derivation of these equations see Appendix A. The noise averages of the neuronal state variables obey

$$\tau_0 \frac{d}{dt}\langle S_i(t)\rangle = -\langle S_i(t)\rangle + \langle g(h_i(t))\rangle , \quad t \geq 0 . \quad (3.4)$$

The correlation between the activities of two neurons is defined as

$$C_{ij}(t, t+\tau) \equiv \langle \delta S_i(t)\delta S_j(t+\tau)\rangle , \quad \tau \geq 0 , \quad (3.5)$$

where $\delta S_i(t) \equiv S_i(t) - \langle S_i(t)\rangle$. The equal-time ($\tau = 0$) correlations obey

$$\tau_0 \frac{d}{dt}C_{ij}(t, t) = -2C_{ij}(t, t) + \langle \delta S_i(t)\delta g(h_j(t))\rangle$$
$$+ \langle \delta S_j(t)\delta g(h_i(t))\rangle , \quad t \geq 0 . \quad (3.6)$$

The time-delayed correlations obey

$$\tau_0 \frac{d}{d\tau}C_{ij}(t, t+\tau) = -C_{ij}(t, t+\tau)$$
$$+ \langle \delta S_i(t)\delta g(h_j(t+\tau))\rangle .$$

$$\tau \geq 0 . \quad (3.7)$$

The equilibrium value of moments that depend on a single time variable is defined by taking the $t \to \infty$ limit, which is equivalent to calculating moments of the equilibrium distribution $P(\{S\}, \infty)$. Thus the average activities obey at equilibrium

$$\langle S_i\rangle = \langle g(h_i)\rangle , \quad (3.8)$$

where the angular brackets mean the average with the equilibrium distribution. Likewise, the equilibrium value of the equal-time correlations, denoted as $C_{ij}(0)$, obey

$$2C_{ij}(0) = \langle \delta S_i \delta g(h_j)\rangle + \langle \delta S_j \delta g(h_i)\rangle . \quad (3.9)$$

The equilibrium value of the time-delayed correlations is defined by taking the limit $t \to \infty$, keeping the delay time τ finite. Thus $C_{ij}(\tau) \equiv \lim_{t\to\infty} C_{ij}(t, t+\tau)$ obeys

$$\tau_0 \frac{d}{d\tau}C_{ij}(\tau) = -C_{ij}(\tau) + \langle \delta S_i(t)\delta g(h_j(t+\tau))\rangle .$$

$$\tau \geq 0 , \quad (3.10)$$

which needs to be solved together with the initial condition given by $C_{ij}(0)$.

In general, the above equations cannot be solved exactly since their right-hand side involves arbitrarily high order moments. Below we will specify a network archi-

tecture for which these equations can be solved exactly in the limit of large networks, as we will show in Sec. VI. It is instructive, however, to consider the simple case of two coupled neurons.

C. Correlations induced by a single connection

We consider the case of an isolated pair of neurons, say, 1 and 2, that are coupled by a connection $J_{21} = J$ from neuron 1 to neuron 2. The connection in the reverse direction J_{12} is assumed to be zero. Thus the instantaneous local fields of the two neurons are

$$h_1(t) = -\theta_1 , \quad (3.11)$$

$$h_2(t) = JS_1(t) - \theta_2 . \quad (3.12)$$

We consider here only the equilibrium limit. The average activities are

$$\langle S_1\rangle = g(-\theta_1) , \quad (3.13)$$

$$\langle S_2\rangle = \langle S_1\rangle \Delta g_2 + g(J - \theta_2) , \quad (3.14)$$

where $\Delta g_2 \equiv g(J-\theta_2)-g(-\theta_2)$. In deriving these results, we have used Eq. (3.8) and the fact that

$$g(JS - \theta) = Sg(J - \theta) + (1 - S)g(-\theta) . \quad (3.15)$$

The equal-time ACs $C_{ii}(0) \equiv \langle (\delta S_i)^2\rangle$ are simply

$$C_{ii}(0) = \langle S_i\rangle(1 - \langle S_i\rangle) . \quad (3.16)$$

Both Eqs. (3.15) and (3.16) are a direct consequence of the fact that $S = 0, 1$. From Eq. (3.9) one obtains, for the equal-time CCs,

$$C_{12}(0) = \frac{1}{2}C_{11}(0)\Delta g_2 . \quad (3.17)$$

The factor $C_{11}(0)$ measures the fluctuations in the activity of neuron 1. The factor Δg_2 measures the response of neuron 2 to these fluctuations.

The time-delayed equations reduce to

$$\tau_0 \frac{d}{d\tau}C_{11}(\tau) = -C_{11}(\tau) , \quad \tau \geq 0 \quad (3.18)$$

$$\tau_0 \frac{d}{d\tau}C_{21}(\tau) = -C_{21}(\tau) , \quad \tau \geq 0 \quad (3.19)$$

$$\tau_0 \frac{d}{d\tau}C_{22}(\tau) = -C_{22}(\tau) + \Delta g_2 C_{21}(\tau) , \quad \tau \geq 0 \quad (3.20)$$

$$\tau_0 \frac{d}{d\tau}C_{12}(\tau) = -C_{12}(\tau) + \Delta g_2 C_{11}(\tau) , \quad \tau \geq 0 . \quad (3.21)$$

Solutions of these equations yield

$$C_{11}(\tau) = C_{11}(0)\exp(-|\tau|/\tau_0) , \quad (3.22)$$

$$C_{21}(\tau) = C_{12}(0)\exp(-\tau/\tau_0) , \quad \tau \geq 0 . \quad (3.23)$$

These decays characterize the effect of the local stochastic noise, assumed in our model. In addition,

$$C_{22}(\tau) = [C_{22}(0) + \Delta g_2 C_{12}(0)|\tau|/\tau_0)]\exp(-|\tau|/\tau_0) , \quad (3.24)$$

$$C_{12}(\tau) = C_{12}(0)(1 + 2\tau/\tau_0)\exp(-\tau/\tau_0) , \quad \tau \geq 0 . \quad (3.25)$$

Note that $C_{12}(\tau) = C_{21}(-\tau)$. Here the time dependence is affected by the interaction J. The results are shown in Fig. 1 for the cases of $g(-\theta_1) = 1/2$, $g(-\theta_2) = 0$, and $g(J - \theta_2) = 1$. As seen in Fig. 1(a), the decay of the AC of neuron 2 is slower than that of neuron 1, due to the excitatory influence of the latter. However, this effect is not large. The asymmetric shape of $C_{12}(\tau)$, seen in Fig. 1(b), is, of course, a manifestation of the unidirectional nature of the interaction between the two neurons. It should be noted, however, that despite the absence of J_{12}, $C_{12}(\tau)$ does not vanish at negative τ, because of the temporal
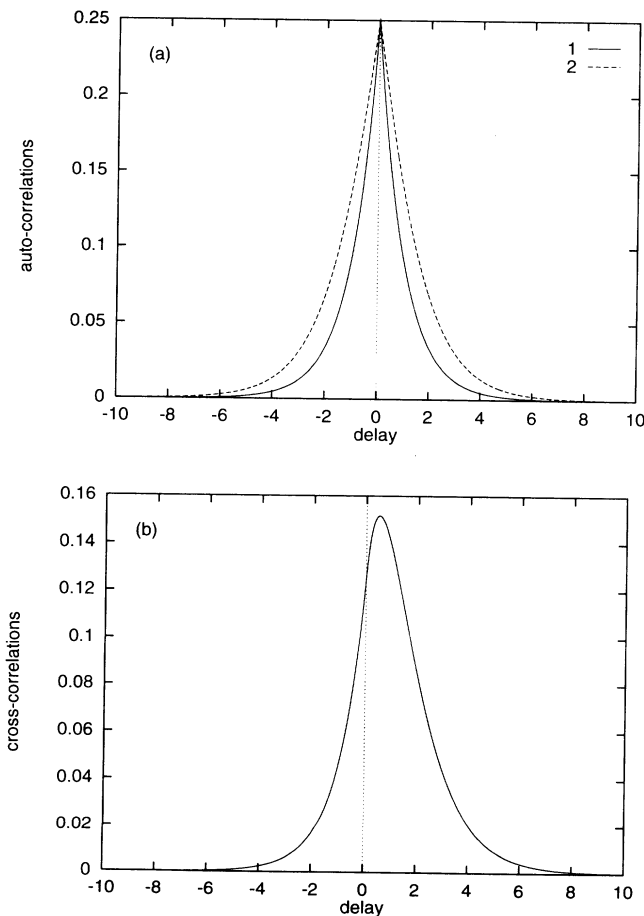

FIG. 1. Correlation functions for an isolated pair of neurons with a unidirectional connection from neuron (1) to neuron (2). (a) Autocorrelations. (b) Cross correlation.

memory in the fluctuations of S_1. Thus, contrary to the common assumption, cross correlations induced by a single synapse are not necessarily "one sided." This is a manifestation of the fact that, unlike response functions, correlation functions are not causal.

D. Network architecture

We study the correlations in fully connected recurrent networks, divided into K subpopulations such that $K \ll N$. The kth population consists of N_k neurons and $N_k \gg 1$. These populations represent naturally cortical columns, but also may correspond to different neuronal types (e.g., excitatory and inhibitory) within a column. We will denote the coordinate of each neuron by a superscript denoting its group index and a subscript denoting its index within the group. Thus the state of the ith neuron in the kth population is denoted as S_k^i and the connection between this neuron and the jth (presynaptic) neuron in the lth population is J_{kl}^{ij}. Note that from now on, subscripts will denote population indices and superscripts intrapopulation indices, unless otherwise specified. An important assumption is that all the connections between presynaptic neurons in the lth group and postsynaptic ones in the kth group are all equal, i.e., $J_{kl}^{ij} = J_{kl}/N_l$, except for the self-coupling J_{kk}^{ii}, which is zero. The scaling of the interactions by the number of neurons in the presynaptic group is required in order to make sure that the total synaptic input from each group is of the order of the local noise (or equivalently of the order of the difference between the resting and threshold potentials). This implies that the individual synaptic efficacies are weak. We will assume that the cellular properties of neurons within a group are uniform, so that except for local stochastic noise the response properties of all the neurons in a group are equal.

With the above assumptions, the local fields of all the neurons in a given population are equal. The local field in, say, the kth population is

$$h_k(t) = \sum_{l=1}^{K} J_{kl} S_l(t) - \theta_k , \quad (3.26)$$

where S_l is the population-averaged activities of the lth group:

$$S_l(t) = \frac{1}{N_l} \sum_{i=1}^{N_l} S_l^i(t) . \quad (3.27)$$

IV. AVERAGE FIRING RATES

The quantities of interest are the dynamics of the population averaged activities $S_l(t)$. We can separate these quantities to noise averages $\langle S_l(t) \rangle$ and fluctuations $\delta S_l \equiv S_l(t) - \langle S_l(t) \rangle$. In a large population δS_l is small, i.e., of the order of $N_l^{-1/2}$. Thus to leading order in $1/N$

the population activities evolve according to the *following equations* (see Appendix A):

$$\tau_0 \frac{d\langle S_k \rangle}{dt} = -\langle S_k \rangle + g \left(\sum_{l=1}^{K} J_{kl} \langle S_l \rangle - \theta_k \right) ,$$

$$k = 1, \ldots, K . \quad (4.1)$$

We refer to these equations as the mean-field equations of the system. Equations of this form have been studied extensively. Depending on the various parameters, the stable solutions of these equations are either fixed points or limit cycles. The fixed-point solutions represent an asynchronous state of the network in which the population-averaged activities are almost constant in time. The limit-cycle solutions represent a synchronous state in which there is a coherent oscillatory activity. Obviously in the latter case there are strong oscillatory correlations among the neurons. Here we study the behavior of asynchronous networks where correlations are the results of irregular fluctuations in activities rather than a globally synchronized dynamical state. The fixed points of the network are described by

$$\tilde{S}_k = g(\tilde{h}_k) , \quad k = 1, \ldots, K , \quad (4.2)$$

where

$$\tilde{h}_k = \sum_{l=1}^{K} J_{kl} \tilde{S}_l - \theta_k , \quad k = 1, \ldots, K . \quad (4.3)$$

The fixed point values $\tilde{S}_k$ has two physical meaning. It represents the value of the population-averaged activity of the kth group, up to corrections of the order of $N_k^{-1/2}$. It is also equal to the *time average* of the activity of any individual neuron in the group. The equivalence of population average and time average is one of the characteristics of asynchronous stochastic homogeneous networks.

The stability of the fixed points is determined by studying the dynamics of a small perturbation about the fixed point. Linearization of the dynamical equations of the perturbations about the fixed point yields

$$\tau_0 \frac{d}{dt} \delta S_k(t) = -\delta S_k(t) + \sum_{l=1}^{K} \tilde{J}_{kl} \delta S_l(t) , \quad (4.4)$$

where $\delta S_k(t) = S_k(t) - \tilde{S}_k$. The matrix $\tilde{J}_{kl}$ is

$$\tilde{J}_{kl} \equiv g_k' J_{kl} . \quad (4.5)$$

where $g_k' \equiv g'(\tilde{h}_k)$ and $g'(h) \equiv dg/dh$. Thus the effective connection $\tilde{J}_{kl}$ is the direct connection between a pair of neurons multiplied by the gain of the postsynaptic neuron. Note that the gain itself depends on the state of the whole system since, in general, it is a function of the the local field $\tilde{h}_k$. From Eq. (4.4) it follows that the fixed-point solution is stable as long as the real part of the eigenvalues of $\tilde{\mathbf{J}}$ and λ_k, is less than 1.

V. DYNAMIC LINEAR RESPONSE

We first use Eq. (4.1) to calculate the linear response of the neurons to an external source. Assume that a small time-dependent source $\delta h_k^i(t)$ is added to the local field acting on the neuron i in the kth population. To compute the changes in the noise-averaged firing rates induced by this source we write

$$\langle S_k^i(t) \rangle = \tilde{S}_k + \sum_{l=1}^{K} \sum_{j=1}^{N_l} \int_0^t dt' \chi_{ik,jl}(t - t') \delta h_l^j(t')$$

$$+ O(\delta h^2) , \quad (5.1)$$

where $\tilde{S}_k$ is the fixed-point solution for $\delta h = 0$. The matrix $\chi(t)$ is the linear response matrix. It is defined as

$$\chi_{ik,jl}(t - t') \equiv \frac{\partial \langle S_k^i(t) \rangle}{\partial h_l^j(t')} , \quad t > t' . \quad (5.2)$$

In the present architecture, χ can be written as

$$\chi_{kl}^{ij}(\tau) = \chi_k(\tau) \delta_{kl} \delta_{ij} + \chi_{kl}(\tau)(1 - \delta_{kl} \delta_{ij}) . \quad (5.3)$$

The first term is the local response. The second term is the nonlocal response within a population (χ_{kk}) and across different populations (χ_{kl}, $k \neq l$). Adding $\delta h_k^i(t)$ to the argument of g on the right-hand side of Eq. (4.1) and linearizing with respect to δh one obtains, for the local response.

$$\chi_k(\tau) = \tau_0^{-1} g_k' \exp(-\tau/\tau_0) , \quad \tau > 0 \quad (5.4)$$

up to corrections of $O(1/N)$. To derive the value of the nonlocal response matrix, we Fourier transform (in time) the linearized equations, yielding, for the Fourier transform of $\chi_{kl}(t)$, the result

$$\chi_{kl}(\omega) = \{ [(1 - i\omega\tau_0)\mathbf{I} - \tilde{\mathbf{J}}]_{kl}^{-1} - (1 - i\omega\tau_0)^{-1} \delta_{kl} \} N_l^{-1} g_l' . \quad (5.5)$$

The subtraction of the last term is due to the fact that χ_{kl} represents only the nonlocal part of the full response matrix. Note that the interaction matrix appearing in this equation is not the full $N \times N$ connection matrix, but is the reduced $K \times K$ matrix corresponding to the effective interactions between the populations. To solve Eq. (5.5) it is useful to introduce the K right eigenvectors $\{\mathbf{R}^\mu\}$ and left eigenvectors $\{\mathbf{L}^\mu\}$ of $\tilde{\mathbf{J}}$, corresponding to the set of K eigenvalues of $\{\lambda_\mu\}$ of $\tilde{\mathbf{J}}$. Throughout this work we assume that the matrix $\tilde{\mathbf{J}}$ is diagonalizable, so that the K right as well as left eigenvectors form a complete set. Thus they satisfy the completeness condition

$$\sum_{\mu=1}^{K} R_k^\mu L_l^\mu = \delta_{kl} \quad (5.6)$$

and can be chosen to obey also the biorthogonality condition

$$\mathbf{R}^{\mu} \cdot \mathbf{L}^{\nu} = \delta_{\mu\nu} \ . \tag{5.7}$$

The response matrix can be decomposed into

$$\chi_{kl}(\omega) = \sum_{\mu=1}^{K} R_k^{\mu} \chi_l^{\mu}(\omega) \ , \tag{5.8}$$

where

$$\chi_l^{\mu}(\omega) = \sum_{k=1}^{K} \chi_{kl}(\omega) L_k^{\mu} \ . \tag{5.9}$$

Using Eq. (5.5) to solve for $\chi_k^{\mu}(\omega)$ one obtains

$$\chi_{kl}(\omega) = g_l' N_l^{-1} \sum_{\mu=1}^{K} R_k^{\mu} L_l^{\mu} \left(\frac{1}{1 - \lambda_{\mu} - i\omega\tau_0} - \frac{1}{1 - i\omega\tau_0} \right) \tag{5.10}$$

or

$$\chi_{kl}(\tau) = \tau_0^{-1} g_l' N_l^{-1} \sum_{\mu=1}^{K} R_k^{\mu} L_l^{\mu} \exp[-\tau(1 - \lambda_{\mu})/\tau_0]$$
$$- \tau_0^{-1} g_l' N_l^{-1} \delta_{kl} \exp(-\tau/\tau_0) \ , \quad \tau > 0 \ . \tag{5.11}$$

The static response is obtained by integrating Eq. (5.11) over all $\tau > 0$ which equals $\chi(\omega = 0)$.

Suppose the source is spatially distributed so that it has the same amplitude $\delta h_l(t)$ at all the sites in the lth population. We define the population linear response matrix as the linear response of the kth population to $h_l(t)$, i.e.,

$$\tilde{\chi}_{kl}(\tau) \equiv \frac{\partial \langle S_k(\tau) \rangle}{\partial h_l(0)} \ . \tag{5.12}$$

It is straightforward to show that

$$\tilde{\chi}_{kl}(\omega) = g_l' \sum_{\mu=1}^{K} \frac{R_k^{\mu} L_l^{\mu}}{1 - \lambda_{\mu} + i\omega\tau_0} \tag{5.13}$$

and the time dependence is simply

$$\tilde{\chi}_{kl}(\tau) = \tau_0^{-1} g_l' \sum_{\mu=1}^{K} R_k^{\mu} L_l^{\mu} \exp[-\tau(1 - \lambda_{\mu})/\tau_0] \ , \quad \tau > 0 \ . \tag{5.14}$$

VI. CORRELATION FUNCTIONS

The time-delayed autocorrelation of a neuron in the kth group is

$$C_k(t, t + \tau) \equiv \langle \delta S_k^i(t) \delta S_k^i(t + \tau) \rangle \ , \tag{6.1}$$

where as before $\delta S_k^i = S_k^i - \langle S_k^i \rangle$ and the angular brackets denote averaging over the stochastic noise. Similarly, the time-delayed CC between neurons in groups k and l is

$$C_{kl}(t, t + \tau) \equiv \langle \delta S_k^i(t) \delta S_l^j(t + \tau) \rangle \ , \quad i, k \neq j, l \ . \tag{6.2}$$

Note that the homogeneity of the groups implies that the correlations do not depend on i and j. The equilibrium value of the correlation-functions is defined as

$$C_k(\tau) \equiv \lim_{t \to \infty} \langle \delta S_k^i(t) \delta S_k^i(t + \tau) \rangle \ , \tag{6.3}$$

$$C_{kl}(\tau) \equiv \lim_{t \to \infty} \langle \delta S_k^i(t) \delta S_l^j(t + \tau) \rangle \ , \quad i, k \neq j, l \ . \tag{6.4}$$

In the long-time limit the noise averaged correlations are equal to the correlations defined by averaging over the absolute time t. Here we will focus on equilibrium values.

We first discuss the value of the AC functions. Using the general result Eq. (3.16), the equal-time ACs are, to zeroth order in $1/N$,

$$C_k(0) = \tilde{S}_k(1 - \tilde{S}_k) \ . \tag{6.5}$$

Using the master equations, Eqs. (3.3), and the network architecture, it can be shown (Appendix B) that, to leading order in $1/N$ the time-delayed ACs obey the same differential equation

$$\tau_0 \frac{d}{d\tau} C_k(\tau) = -C_k(\tau) \tag{6.6}$$

as in the noninteracting case, yielding

$$C_k(\tau) = \tilde{S}_k(1 - \tilde{S}_k) \exp(-|\tau|/\tau_0) \ . \tag{6.7}$$

Thus, to leading order the decay of the ACs is dominated purely by the local noise and is unaffected by the interactions. The $O(1/N)$ correction to the ACs will be evaluated below.

Next, we consider the equal-time CCs. The differential equation for the nonequilibrium CC, $\mathbf{C}(t, t)$, is described in Appendix B. Here we focus on the values of the equal-time CCs at equilibrium, i.e., $\mathbf{C}(\tau = 0)$. This matrix obeys the linear equation

$$2\mathbf{C}(0) = \mathbf{C}(0)\tilde{\mathbf{J}}^T + \tilde{\mathbf{J}}\mathbf{C}(0) + \mathbf{A}(0) + \mathbf{A}^T(0) \ , \tag{6.8}$$

where $\tilde{J}$ is the effective interaction matrix Eq. (4.5) and the superscript T stands for the transpose of a matrix. The matrix $\mathbf{A}(\tau)$ is defined by

$$A_{kl}(\tau) \equiv N_k^{-1} C_k(\tau) \tilde{J}_{lk} \ , \tag{6.9}$$

where $C_k(\tau)$ are given by Eq. (6.7). Note that the ACs act like a "source" for the CCs.

Equation (6.8) can be solved efficiently using the eigenvectors of $\tilde{\mathbf{J}}$. We define

$$C_{\mu\nu} = \mathbf{L}^{\mu} \cdot \mathbf{C}(0)\mathbf{L}^{\nu} \tag{6.10}$$

and similarly

$$A_{\mu\nu} = \mathbf{L}^{\mu} \cdot \mathbf{A}(0)\mathbf{L}^{\nu} \ , \tag{6.11}$$

where Eq. (6.9) implies

$$A_{\mu\nu} = \lambda_\nu \sum_{k=1}^{K} L_k^\mu L_k^\nu N_k^{-1} C_k(0) \quad . \tag{6.12}$$

By multiplying Eq. (6.8) both from the right and the left by left eigenvectors one obtains

$$C_{\mu\nu} = \frac{A_{\mu\nu} + A_{\nu\mu}}{2 - \lambda_\mu - \lambda_\nu} \quad . \tag{6.13}$$

The full equal-time CC matrix is expressed in terms of these coefficients via the expansion

$$C_{kl}(0) = \sum_{\mu,\nu=1}^{K} R_k^\mu R_l^\nu C_{\mu\nu} \quad . \tag{6.14}$$

The time-delayed CC matrix $\mathbf{C}(\tau)$ obeys (Appendix B) the first-order linear differential equation

$$\tau_0 \frac{d}{d\tau} \mathbf{C}(\tau) = -\mathbf{C}(\tau)(\mathbf{I} - \tilde{\mathbf{J}}^T) + \mathbf{A}(\tau) \quad , \quad \tau \geq 0 \quad . \tag{6.15}$$

This equation, together with its initial condition given by the equal-time correlation matrix Eq. (6.8), completely specifies the time-delayed correlations. We define

$$C_{kl}(\tau) = \sum_{\mu=1}^{K} C_k^\mu(\tau) R_l^\mu \quad . \tag{6.16}$$

where

$$C_k^\mu(\tau) = \sum_{l=1}^{K} C_{kl}(\tau) L_l^\mu \quad . \tag{6.17}$$

Similarly

$$A_{kl}(\tau) = \sum_{\mu=1}^{K} A_k^\mu(\tau) R_l^\mu \quad , \tag{6.18}$$

where according to Eq. (6.9)

$$A_k^\mu(\tau) = \lambda_\mu N_k^{-1} C_k(\tau) L_k^\mu \quad . \tag{6.19}$$

Equation (6.15) yields $\tau_0 dC_k^\mu/d\tau + (1 - \lambda_\mu)C_k^\mu = A_k^\mu$, which leads to

$$C_{kl}(\tau) = \sum_{\nu=1}^{K} [C_k^\nu(0) + N_k^{-1} C_k(0) L_k^\nu] R_l^\nu$$
$$\times \exp[-\tau(1 - \lambda_\nu)/\tau_0]$$
$$-\delta_{kl} N_k^{-1} C_k(0) \exp(-\tau/\tau_0) \quad , \quad \tau \geq \tau_0 \quad . \tag{6.20}$$

The quantity $C_k^\nu(0)$ is given by Eq. (6.17) at $\tau = 0$, which, by Eq. (6.14), equals

$$C_k^\nu(0) = \sum_{\mu=1}^{K} R_k^\mu C_{\mu\nu} \quad . \tag{6.21}$$

Having calculated the CCs we can evaluate the $O(1/N)$ corrections to the ACs. It can be shown (Appendix B) that

$$\tau_0 \frac{d}{d\tau} C_k(\tau) = -C_k(\tau) + [\mathbf{C}(\tau)\tilde{\mathbf{J}}^T]_{kk} \quad + \quad O(1/N^2) \quad ,$$
$$\tau \geq 0 \quad . \tag{6.22}$$

Thus the solution for the ACs up to order $1/N^2$ is

$$C_k(\tau) = C_k(0)[1 - |\tau|\tilde{J}_{kk}/(\tau_0 N_k)] \exp(-|\tau|/\tau_0)$$
$$+ \sum_{\nu=1}^{K} [C_k^\nu(0) + N_k^{-1} C_k(0) L_k^\nu]$$
$$\times \exp(-|\tau|/\tau_0)[\exp(|\tau|\lambda_\nu) - 1] \quad . \tag{6.23}$$

Since the CCs are of order $O(1/N)$, they add a correction of this order to the ACs. This correction is negligible except near a bifurcation point as will be shown in Sec. VII.

Finally, it should be noted that the above theory predicts a marked difference between the short-time properties of the ACs and the CCs. According to Eq. (6.23) the ACs have a cusp at $\tau = 0$, whereas the CCs which integrate the ACs' time dependence [see Eq. (6.15)] do not have a cusp at any τ, i.e., $\dot{C}_{kl}(\tau)$ is continuous. In particular, the diagonal element C_{kk} is an even function of τ; hence $\dot{C}_{kk}(0) = 0$. This difference is illustrated in the example presented in Sec. IX.

A. Decomposition of an observed correlation matrix

So far we have discussed the form of the correlations and linear response functions assuming that the interactions between the different populations (and the gain parameters) are known. In many cases the converse situation exists. One would like to infer about the underlying connectivity from experimentally measured correlations or responses. We will briefly discuss the decomposition of the correlation matrix. Similar considerations apply for the response functions.

In general, the equal-time correlation matrix as well as the average rates and gains do not contain sufficient information for the unique determination of the interaction matrix $\mathbf{J}$. However, in principle one can use the time dependence of $\mathbf{C}$ to decompose it to the underlying fundamental nonorthogonal modes. According to the result of Eq. (6.20), the decay of the correlation can be decomposed to up to $K + 1$ terms, each of which is decaying as a single exponential. Let us order the eigenvalues in a decreasing order of their real values λ_μ', so that $\lambda_1' \geq \lambda_2' \geq \lambda_3' \geq \cdots$ and define $\lambda_0 \equiv 0$, representing the last term in Eq. (6.20). Suppose we can decompose the experimentally measured $C_{kl}(\tau)$ into

$$C_{kl}(\tau) = \sum_{\nu} C_{kl}^{(\nu)} \exp(-\tau\omega_\nu) \quad . \tag{6.24}$$

Note that $C_{kl}^{(\nu)}$ can be complex if ω_ν is complex. Then according to Eq. (6.20) the matrix $C_{kl}^{(\nu)}$ is expected to be of the form $C_{kl}^{(\nu)} \approx \tilde{C}_k^\nu R_l^\nu + \eta_{kl}^\nu$ where $\tilde{C}_k^\nu = C_k^\nu(0) + N_k^{-1} C_k(0) L_k^\nu$ and the second term represents some noise, e.g., from imprecise measurements of the correlations. An estimate of the vector $\mathbf{R}^\nu$ can be computed

by minimizing

$$\sum_{k,l=1}^{K} |C_{kl}^{(\nu)} - \tilde{C}_k^\nu R_l^\nu|^2 \qquad (6.25)$$

with respect to the pair of vectors $\mathbf{R}^\nu$ and $\tilde{\mathbf{C}}^\nu$ subject to appropriate normalization convention. The optimal estimate for $\mathbf{R}^\nu$ is given by the eigenvector with the largest eigenvalue of the (Hermitian) matrix $\mathbf{C}^{(\nu)T}\mathbf{C}^{(\nu)*}$, where the asterisk stands for the complex conjugate. The corresponding eigenvalue of the matrix $\tilde{\mathbf{J}}$ is given by the decay constant ω_ν through $\lambda_\nu \propto \tau_0^{-1} - \omega_\nu$. In practice, this decomposition is feasible only if there are few dominant exponential decays. In particular, if there is a significant gap between the slowest decay rate ω_1 and the rest, then by considering the long-time part of $C_{kl}(\tau)$ one should be able to identify the eigenvector of $\tilde{J}$ with the smallest (real part of) eigenvalue.

VII. AMPLIFICATION OF FLUCTUATIONS NEAR A BIFURCATION POINT

One of the main consequences of the above results is concerned with the behavior of the correlations near a bifurcation point. This occurs when the parameters of the system are such that the real part of one of the eigenvalues of $\tilde{J}$ becomes close to 1. Our analysis shows that in this case, the system will exhibit anomalously large fluctuations about the (stable) fixed point and the fluctuations will have an anomalously long correlation time.

Let us suppose that the system is near a saddle-node bifurcation, which is characterized by a single critical mode [22]. In this case, at the bifurcation point, $\lambda_1 = 1$ while $\lambda_\nu' < 1$ for $\nu > 1$. According to Eqs. (6.10)–(6.14), as the bifurcation point is approached, both the amplitude and the decay time of $C_{11}(\tau)$ will diverge as ϵ^{-1} where $\epsilon \equiv 1 - \lambda_1$. Thus, if the system is sufficiently close to the bifurcation point, we can approximate the correlation matrix by

$$C_{kl}(\tau) \propto \frac{R_k^1 R_l^1}{N\epsilon} \exp(-\tau\epsilon/\tau_0) , \quad \tau \geq 0. \qquad (7.1)$$

Another common bifurcation point is a Hopf bifurcation where there is a pair of complex conjugate eigenvalues λ_1 and λ_2 such that $\lambda_1 = 1 - \epsilon + i\omega_1\tau_0$ and $\lambda_2 = 1 - \epsilon - i\omega_1\tau_0$, and $\omega_1\tau_0 > 0$ at the bifurcation point where $\epsilon \to 0$. Near such a point, the dominant contribution to $\mathbf{C}$ comes from C_{12} and C_{21}, as follows from Eq. (6.13). Taking into account this contribution, the correlations will exhibit weakly damped oscillations of the form

$$C_{kl}(\tau) \propto \frac{|R_k^1 R_l^2|}{N\epsilon} \cos(\omega_1\tau + \phi_{kl}) \exp(-\tau\epsilon/\tau_0) , \quad \tau \geq 0 ,$$
$$(7.2)$$

where $\phi_{kl} = \phi + \phi_k - \phi_l$ and ϕ_k and ϕ_l are the phases of R_k^1 and R_l^2, respectively.

In practice, the approximations of Eqs. (7.1) and (7.2) may not be good at short times because of the contributions of many noncritical modes, which may be significant if ϵ is not too small. On the other hand, because these modes decay fast, the above approximations will be good for the intermediate- or long-time behavior of $\mathbf{C}$.

In any finite system the pairwise CCs cannot diverge since they are averages of finite quantities. Hence the implication of the above predictions for a large but finite system needs to be clarified. Since the above analysis was confined to the leading [i.e., $O(1/N)$] contributions to the CCs, the divergence of the theoretical expressions for the CCs means that near the bifurcation, the CCs are not of order $1/N$ but are much larger than that. The actual magnitude of the equal-time CCs at the bifurcation point depends on the nature of the bifurcation. On the basis of finite-size scaling arguments [23,24] it is expected that at a saddle-node bifurcation or a supercritical Hopf bifurcation the correlations grow to

$$\mathbf{C}(0) \sim 1 , \quad \epsilon \approx 0 . \qquad (7.3)$$

On the other hand, it is expected that a subcritical Hopf bifurcation, the correlations grow only to

$$\mathbf{C}(0) \sim 1/\sqrt{N} , \quad \epsilon \approx 0 . \qquad (7.4)$$

The instability at the bifurcation point will also show up in the nonlocal linear response. Near a saddle-node bifurcation, the response at long time is, according to Eq. (5.11),

$$\chi_{kl}(\tau) \approx \tau_0 g_l' N_l^{-1} R_k^1 L_l^1 \exp(-\tau\epsilon/\tau_0) , \quad \tau\epsilon/\tau_0 \geq 1 \qquad (7.5)$$

and the static response is

$$\chi_{kl} \approx \frac{g_l' N_l^{-1} R_k^1 L_l^1}{\epsilon} . \qquad (7.6)$$

Likewise, near a Hopf bifurcation the long-time behavior of χ is

$$\chi_{kl}(\tau) \approx \tau_0^{-1} g_l' N_l^{-1} |R_k^1 L_l^2| \cos(\omega_1\tau + \phi_{kl})$$
$$\times \exp(-\tau\epsilon/\tau_0) , \quad \tau\epsilon/\tau_0 \geq 1 . \qquad (7.7)$$

Note that in the case of a Hopf bifurcation, the static response matrix is not dominated by the critical mode. Instead, the critical mode will show up as a resonance in the frequency-dependent χ at $\omega = \pm\omega_1$, i.e.,

$$\chi_{kl}(\omega) \approx \frac{g_l' N_l^{-1} R_k^1 L_l^2}{\epsilon - i(\omega - \omega_1)\tau_0} , \quad \omega \approx \omega_1 \qquad (7.8)$$

and similarly for $\omega \approx -\omega_1$.

VIII. NETWORKS WITH RANDOM CONNECTIONS

So far we have assumed that the network is microscopically homogeneous, meaning that the properties of neurons within each populations are the same and that the interactions between pairs of neurons depend only

on the identity of their populations. Since realistic neural networks contain a significant level of inhomogeneity, it is important to extend our results to inhomogeneous networks. Here we will consider only inhomogeneity generated by randomizing the connections. Specifically, we assume that the connections J_{kl}^{ij} are independent random variables, of the order of $1/N_l$, with means J_{kl}/N_l, which can also be defined via

$$J_{kl} = \sum_{j=1}^{N_l} J_{kl}^{ij} . \qquad (8.1)$$

Except for this randomness the network has the same architecture as before and in particular the local parameters, such as thresholds, are homogeneous within a population. Under the above conditions, the local field acting upon S_k^i is still given by $h_k^i = \sum_{l=1}^{K} J_{kl}\langle S_l \rangle - \theta_k$. Thus the noise-averaged firing rates of single neurons are equal to the population-averaged firing rates. Both obey the homogeneous dynamics, given by Eq. (4.1). In particular, the average rates in the asynchronous states Eq. (4.2) as well as the ACs, Eq. (6.5) will be the same as those of a homogeneous network with the same J_{kl}. This is because the inhomogeneity is only in the connections and not in the local properties.

The randomness of the connections will clearly affect the CCs because the CC between a pair of neurons has also a contribution from the direct connection between them. Although this contribution is small in absolute terms, it is of the same order as the contribution of their common synaptic input; hence it cannot be neglected. We define the full matrix of equal-time CCs by

$$C_{kl}^{ij}(0) = \langle \delta S_k^i(t)\delta S_l^j(t)\rangle, \quad i,k \neq j,l . \qquad (8.2)$$

Using the general result of Appendix B [Eq. (B8)] we obtain, in our case,

$$2C_{kl}^{ij}(0) = \sum_m C_{km}(0)\tilde{J}_{lm} + \sum_m \tilde{J}_{km}C_{ml}(0)$$
$$+ A_{kl}^{ij}(0) + A_{lk}^{ji}(0) , \qquad (8.3)$$

where $C_{kl}(0) \equiv \frac{1}{N_k N_l}\sum_i^{N_k}\sum_j^{N_l} C_{kl}^{ij}(0)$ are the population averaged CCs, $\tilde{J}_{km} = g_k' J_{kl}$ are the average effective connections [see Eq. (8.1] and

$$A_{kl}^{ij}(\tau) = C_k(\tau)g_l' J_{lk}^{ji} . \qquad (8.4)$$

By averaging over the kth and lth populations, we obtain for $C_{kl}(0)$ the same equation as in the homogeneous case Eq. (6.8). In order to evaluate the contribution from the direct interaction, we define $\delta C_{kl}^{ij}(\tau) \equiv C_{kl}^{ij}(\tau) - C_{kl}(\tau)$. By subtracting Eq. (6.8) from Eq. (8.3) we find

$$\delta C_{kl}^{ij}(0) = \frac{1}{2}[\delta A_{kl}^{ij}(0) + \delta A_{lk}^{ji}(0)] , \qquad (8.5)$$

where

$$\delta A_{kl}^{ij}(\tau) = C_k(\tau)g_l'(J_{lk}^{ji} - N_k^{-1}J_{lk}) . \qquad (8.6)$$

Similarly, the population-averaged time-delayed CCs obey the same equation as Eq. (6.15). By subtracting this equation from that of the unaveraged CCs, we find

$$\tau_0\frac{d}{d\tau}\delta C_{kl}^{ij}(\tau) = -\delta C_{kl}^{ij}(\tau) + \delta A_{kl}^{ij}(\tau), \quad \tau \geq 0 . \qquad (8.7)$$

Solving this equation yields

$$\delta C_{kl}^{ij}(\tau) = \delta C_{kl}^{ij}(0) \times \begin{cases} [1 + (\tau/\tau_0)P_{kl}^{ij}]\exp(-\tau/\tau_0) , \\ \qquad\qquad\qquad \tau \geq 0 \quad (8.8) \\ [1 + (|\tau|/\tau_0)(2 - P_{kl}^{ij})] \\ \times \exp(-|\tau|/\tau_0) , \quad \tau \leq 0 . \\ \qquad\qquad\qquad\qquad (8.9) \end{cases}$$

where

$$P_{kl}^{ij} = 2 - P_{lk}^{ji} = \frac{2\delta A_{kl}^{ij}(0)}{\delta A_{kl}^{ij}(0) + \delta A_{lk}^{ji}(0)} . \qquad (8.10)$$

Note that all terms in the above equations are of $0(1/N)$, implying that the fluctuations in the CCs are of the same order as their averages. The quantities P_{kl}^{ij} and P_{lk}^{ji} measure the relative effective strengths of the two direct connections J_{kl}^{ij} and J_{lk}^{ji}, respectively. If $P_{kl}^{ij} \neq 1$, $\delta C_{kl}^{ij}(\tau)$ exhibits an asymmetric shape about the origin. Its shape depends on the value of P_{kl}^{ij}, as will be demonstrated in the example below. If $P_{kl}^{ij} = 1$, then $\delta C_{kl}^{ij}(\tau)$ is symmetric about the origin and except for an overall amplitude is independent of the value of the direct reciprocal connection between the neurons.

As a concrete example of the above results we consider the important case of randomly diluted connectivity matrix. We assume that a connection from the ith neuron in the kth population onto the jth neuron of the lth population exists with a probability $0 \leq f_{kl} \leq 1$. All nonzero connections between neurons of a given pair of populations have the same strength. We can therefore denote the coupling between arbitrary pairs as

$$J_{kl}^{ij} = \frac{J_{kl}}{N_l}\frac{\eta_{kl}^{ij}}{f_{kl}} , \qquad (8.11)$$

where η_{kl}^{ij} are independent random variables which are 1 with probabilities f_{kl} and 0 otherwise.

For simplicity, we consider the case of a pair of neurons within the kth population, say, S_k^i, S_k^j, $i \neq j$. The value of the CC between them depends on whether there are direct connections between them. In the following we present the results for the difference between their CC and the population averaged value $C_{kk}(\tau)$. The population subscript k will be suppressed.

Reciprocally connected pair: $\tilde{J}^{ij} = \tilde{J}^{ji} = N^{-1}\tilde{J} \neq 0$. In this case, $\delta A^{ij}(0) = \delta A^{ji}(0) = \delta C^{ij}(0)$, where

$$\delta C^{ij}(0) = N^{-1}C^{ii}(0)\tilde{J}(f^{-1} - 1) . \qquad (8.12)$$

Hence

$$\delta C^{ij}(\tau) = \delta C^{ij}(0)(1 + |\tau|/\tau_0)\exp(-|\tau|/\tau_0) . \qquad (8.13)$$

Disconnected pair: $\tilde{J}^{ij} = \tilde{J}^{ji} = 0$. In this case, $\delta A^{ij}(0) = \delta A^{ji}(0) = \delta C^{ij}(0)$, where

$$\delta C^{ij}(0) = -N^{-1}C^{ii}(0)\tilde{J} \qquad (8.14)$$

and the time dependence is the same as in Eq. (8.13).

Unidirectional connection: $\tilde{J}^{ji} \neq 0$ but $\tilde{J}^{ij} = 0$. Here $\delta A^{ij}(0) = N^{-1}C^{ii}(0)\tilde{J}(f^{-1} - 1)$ and $\delta A^{ji}(0) = -N^{-1}C^{ii}(0)\tilde{J}$, yielding

$$P^{ij} = \frac{2(1-f)}{1-2f} \ , \quad P^{ji} = \frac{-2f}{1-2f} \ . \qquad (8.15)$$

Hence

$$\delta C^{ij}(0) = \frac{C^{ii}(0)\tilde{J}}{N}\left(\frac{1}{2f} - 1\right) \qquad (8.16)$$

and

$$\delta C^{ij}(\tau) = \delta C^{ij}(0)\left(1 + \frac{2(1-f)}{1-2f}\frac{\tau}{\tau_0}\right)\exp(-\tau/\tau_0) \ ,$$

$$\tau \geq 0 \quad (8.17)$$

$$\delta C^{ij}(-\tau) = \delta C^{ij}(0)\left(1 - \frac{2f}{1-2f}\frac{|\tau|}{\tau_0}\right)\exp(-|\tau|/\tau_0) \ ,$$

$$\tau \leq 0 \ . \quad (8.18)$$

Let us assume for concreteness that the population is excitatory one. Then, the CC is enhanced relative to the average value in the reciprocally connected case and suppressed in the disconnected case. The most interesting case is the unidirectionally connected pair. The nature of δC^{ij} depends on the value of f: if $f \ll 1$ and in particular on whether f is smaller or larger than $1/2$. If $f < 1/2$, $\delta C^{ij}(\tau)$ has a positive value and a positive slope at the origin. It has a maximum at $\tau = \tau_0/[2(1-f)]$ and a minimum at $\tau = -\tau_0/(2f)$. An example is shown in Fig. 2(a), where all three types of δC^{ij} are presented for $f = 0.3$. As can be seen, the unidirectional δC^{ij} is positive at $\tau > 0$, reflecting the contribution of the excitatory connection J^{ji}. On the other hand, it is negative for large negative τ, reflecting the effect of the missing connection J^{ij}. The negative part is, however, relatively small in magnitude. This is because when $f < 1/2$, the existing connection has a stronger effect than the missing one. For the same reason, δC^{ij} is positive also for negative τ near 0. Likewise, the magnitude of the positive δC^{ij} in the reciprocally connected case is larger than that of the negative one for the disconnected case.

The converse is true for $f > 1/2$. In fact, the above equations imply, for the unidirectional case,

$$\delta C^{ij}(\tau \ , \ f) \propto -\delta C^{ij}(-\tau \ , 1 - f) \ . \qquad (8.19)$$

An example is shown in Fig. 2(b). Finally, in the unidirectional case with $f = 1/2$ we have, according to the above results,

$$\delta C^{ij}(\tau) = -\delta C^{ij}(-\tau) \ , \qquad (8.20)$$

as shown in Fig. 2(c). This property reflects the fact

that at $f = 1/2$, the positive effect of the presence of J^{ji} is identical in magnitude to the negative effect of the absence of J^{ij}. Finally, it should be emphasized that the full CCs will depend on δC^{ij} as well as on the population average of the CCs, and thus may depend on the
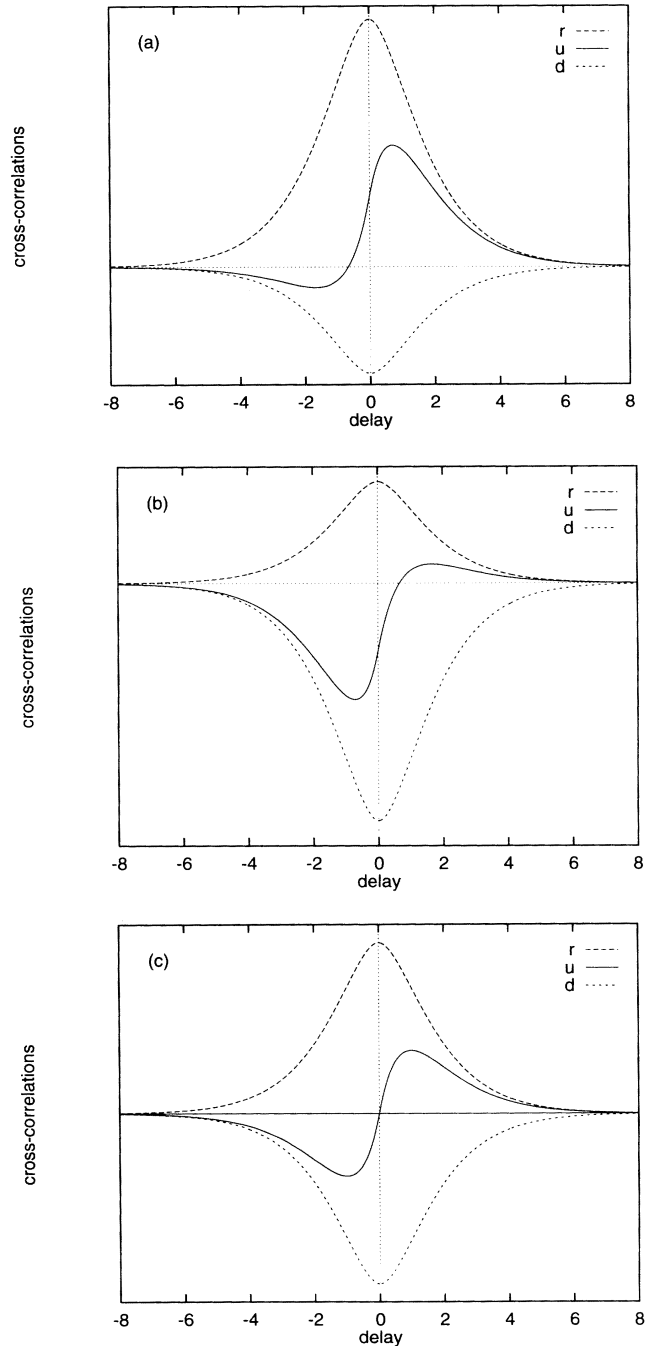

FIG. 2. The cross correlations of a pair of excitatory neurons in a randomly diluted network, with a connection probability f. The population-averaged cross correlations have been subtracted. The vertical scale is arbitrary. Reciprocally connected (r), unidirectionally connected (u), and disconnected (d) pairs are shown. (a) $f = 0.3$. (b) $f = 0.7$. (c) $f = 0.5$.

network architecture and dynamics. This will be discussed in the following section in the context of a specific network model.

IX. NETWORK OF EXCITATORY AND INHIBITORY POPULATIONS

A. Model

In order to demonstrate in detail the general theory, we study a recurrent network that is comprised only of two different populations. One population consists of N_E excitatory neurons, denoted by S_E^j, $j = 1, \ldots, N_E$. The second population consists of N_I inhibitory neurons, denoted by S_I^j, $j = 1, \ldots, N_I$. The network is randomly diluted. The mean excitatory connection between the excitatory neurons equals J_{EE}/N_E. The mean excitatory connection from the excitatory neurons to the inhibitory neurons is J_{IE}/N_E. Similar definitions hold for the inhibitory connections J_{II}/N_I and J_{EI}/N_I, both of which are negative. A diagram of this network is shown in Fig. 3. Each of the neurons is exposed to local noise, which results in stochastic dynamics that is expressed in terms of transition probabilities between the possible states of the neuron, as earlier described in Eq. (3.1). The explicit gain function $g(h)$ is chosen to be a sigmoidal function of the local field

$$g(h) = \frac{1}{2}[1 + \tanh(\beta h)] , \qquad (9.1)$$

where the local field is the sum over all synaptic inputs as defined in Eq. (3.26) and β is the local noise.

Networks similar to the present one have been studied previously, mainly in the context of the possible generation of coherent oscillations [25,26,6,10]. Here we focus on the case of a stable fixed point with low rates. There are two population-averaged activities S_E, S_I for excitatory and inhibitory populations, respectively. On the basis of the equations for the population averages, which were derived earlier for the general case [Eq. (4.1)], we find that the equations describing the fixed points of the population-averaged activities in this case are

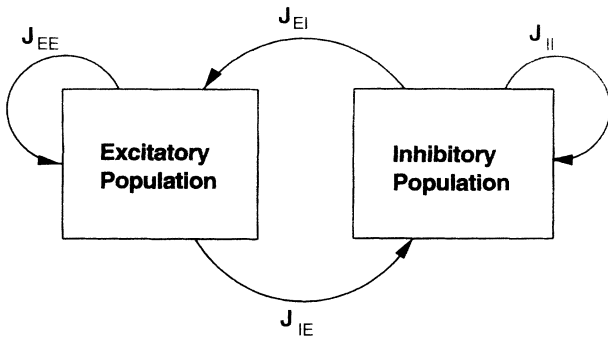$$\tilde{S}_E = \frac{1}{2}\{1 + \tanh\beta[J_{EE}\tilde{S}_E + J_{EI}\tilde{S}_I - \theta]\} , \qquad (9.2)$$

FIG. 3. Schematic connectivity diagram of a network with excitatory and inhibitory populations.

$$\tilde{S}_I = \frac{1}{2}\{1 + \tanh\beta[J_{IE}\tilde{S}_E + J_{II}\tilde{S}_I - \theta]\} . \qquad (9.3)$$

In general, we are interested in locally stable fixed points, which correspond to an asynchronous state of the network. Starting at a fixed point, stability of the network implies that under a small perturbation $\delta S_k(t) = S_k(t) - \tilde{S}_k$ the network will return to its original fixed point. The dynamics of these small perturbations is described by

$$\tau_0\frac{d}{dt}\begin{pmatrix} \delta S_E(t) \\ \delta S_I(t) \end{pmatrix} = -\begin{pmatrix} 1 - \tilde{J}_{EE} & -\tilde{J}_{EI} \\ -\tilde{J}_{IE} & 1 - \tilde{J}_{II} \end{pmatrix}\begin{pmatrix} \delta S_E(t) \\ \delta S_I(t) \end{pmatrix} . \qquad (9.4)$$

where

$$\tilde{J}_{EE} = 2\tilde{S}_E(1 - \tilde{S}_E)\beta J_{EE} . \qquad (9.5)$$

$$\tilde{J}_{II} = 2\tilde{S}_I(1 - \tilde{S}_I)\beta J_{II} . \qquad (9.6)$$

$$\tilde{J}_{EI} = 2\tilde{S}_E(1 - \tilde{S}_E)\beta J_{EI} . \qquad (9.7)$$

$$\tilde{J}_{IE} = 2\tilde{S}_I(1 - \tilde{S}_I)\beta J_{IE} . \qquad (9.8)$$

The eigenvalues of the matrix $\tilde{\mathbf{J}}$ are

$$\lambda_\pm = \frac{\tilde{J}_{EE} + \tilde{J}_{II}}{2} \pm \frac{\sqrt{(\tilde{J}_{EE} - \tilde{J}_{II})^2 + 4\tilde{J}_{EI}\tilde{J}_{IE}}}{2} \qquad (9.9)$$

and the perturbations will decay as long as the real parts of $\lambda_\pm$ do not exceed 1. The right and the left eigenvectors of this matrix are, respectively,

$$R^\pm = \frac{1}{\sqrt{\tilde{J}_{EI}\tilde{J}_{IE} + (\lambda_\pm - \tilde{J}_{EE})^2}}\begin{pmatrix} \tilde{J}_{EI} \\ \lambda_\pm - \tilde{J}_{EE} \end{pmatrix} . \qquad (9.10)$$

$$L^\pm = \frac{1}{\sqrt{\tilde{J}_{IE}\tilde{J}_{EI} + (\lambda_\pm - \tilde{J}_{EE})^2}}\begin{pmatrix} \tilde{J}_{IE} \\ \lambda_\pm - \tilde{J}_{EE} \end{pmatrix} . \qquad (9.11)$$

The projection of a general perturbation on the two left eigenvectors $L^\pm$ decay exponentially with (complex) rates $\lambda^\pm/\tau_0$, respectively.

There are two types of autocorrelations $C_E(\tau)$ and $C_I(\tau)$ for the excitatory and inhibitory neurons, respectively. The equal-time autocorrelations are, to leading order, $C_E(0) = \tilde{S}_E(1 - \tilde{S}_E)$ for the excitatory neurons and $C_I(0) = \tilde{S}_I(1 - \tilde{S}_I)$ for the inhibitory neurons. To leading order of $1/N$, the time-delayed autocorrelations are

$$C_E(\tau) = \tilde{S}_E(1 - \tilde{S}_E)\exp(-|\tau|/\tau_0) , \qquad (9.12)$$

$$C_I(\tau) = \tilde{S}_I(1 - \tilde{S}_I)\exp(-|\tau|/\tau_0) . \qquad (9.13)$$

We denote by $C_{EE}(0)$ the equal-time CCs between two excitatory neurons and similarly for $C_{II}(0)$ and $C_{EI}(0) =$

$C_{IE}(0)$. Using Eq. (6.8), these quantities obey the linear equations

$$(1 - \tilde{J}_{EE})C_{EE}(0) - \tilde{J}_{EI}C_{IE}(0) = \frac{\tilde{J}_{EE}}{N_E}C_E(0) , \quad (9.14)$$

$$(1 - \tilde{J}_{II})C_{II}(0) - \tilde{J}_{IE}C_{IE}(0) = \frac{\tilde{J}_{II}}{N_I}C_I(0) , \quad (9.15)$$

and

$$\left(1 - \frac{1}{2}(\tilde{J}_{EE} + \tilde{J}_{II})\right)C_{IE}(0)$$

$$-\frac{1}{2}\tilde{J}_{EI}C_{EE}(0) - \frac{1}{2}\tilde{J}_{IE}C_{EE}(0)$$

$$= \frac{1}{2N_E}\tilde{J}_{IE}C_E(0) + \frac{1}{2N_I}\tilde{J}_{EI}C_I(0) . \quad (9.16)$$

These equations can be solved directly or by using the general result Eq. (6.14); see Appendix C.

On the basis of Eq. (6.20), we find the solution to the time-delayed CCs which is of the form

$$C_{kl}(\tau) = a_{kl}^+ \exp\left(-\frac{\tau(1 - \lambda_+)}{\tau_0}\right)$$

$$+a_{kl}^- \exp\left(-\frac{\tau(1 - \lambda_-)}{\tau_0}\right) + a_{kl}^0 \exp\left(\frac{-\tau}{\tau_0}\right) ,$$

$$\tau \geq 0 . \quad (9.17)$$

Expressions for the coefficients a_{kl} are given in Appendix C. When $\lambda_\pm$ are real, there are three decaying exponents in the time-delayed CCs, corresponding to two cooperative time constants $\tau_0/[1 - \text{Re}(\lambda_\pm)]$ and one local time constant τ_0. The coefficients a_{kl}^+ will diverge when a saddle-node bifurcation will be reached, i.e., when $\text{Re}(\lambda_\pm) \to 1$. When $\lambda_\pm$ are complex, the cross correlations will exhibit damped oscillations, with frequency of $\text{Im}(\lambda_\pm)/\tau_0$. In this case, for each C_{kl}, both coefficients $a_{kl}^\pm$ diverge when a Hopf bifurcation is approached.

Before we discuss in detail the solution of the above equations we present the simple case of a single homogeneous population, which can be considered as a special case of the present model in which the two populations are not interacting, i.e., $J_{EI} = J_{IE} = 0$. The equal-time CC is simply

$$C_{EE}(0) = \frac{\tilde{J}_{EE}C_E(0)}{N_E(1 - \tilde{J}_{EE})} . \quad (9.18)$$

This expression is a generalization of the well known result for the correlations in an infinite-ranged Ising ferromagnet. For the time dependence, one obtains

$$C_{EE}(\tau) = C_{EE}(0)\exp(-\tau/\tau_0)$$

$$+\frac{C_E(0)}{N_E}\{\exp[-(1 - \tilde{J}_{EE})\tau/\tau_0]$$

$$-\exp(-\tau/\tau_0)\} . \quad (9.19)$$

In this case, the time dependence consists of two pure

exponentials, corresponding to local fluctuations (with decay time τ_0) and a collective, spatially uniform fluctuation [with decay time $\tau_0/(1 - \tilde{J}_{EE})$]. Similar results hold, of course, for an inhibitory population.

B. Choice of parameters

In order to calculate the correlation functions we have to determine the network parameters. Here we use the excitatory-inhibitory network as a crude model for local circuits in the cortex. Since we have not specified any interesting external input, our model corresponds to the background activity of cortical neurons. To be concrete we will determine the parameters on the basis of the available anatomical and physiological estimates on rat cortex. The population-averaged activities in the model represent the ratio between the average firing rate of the physiological neurons and their maximal firing rate. The average background firing rate of cortical neurons in the rat, denoted by ρ, is in the range of 5–10 Hz, while their maximal firing rate, denoted by $\rho_{\max}$, is estimated as 500 Hz. The inhibitory neurons are presumed to have higher rates than the excitatory ones. We therefore choose the average firing rates in the model to be $\langle S_E \rangle = 0.01$ and $\langle S_I \rangle = 0.03$. We set the number of the excitatory neurons in the network to $N_E = 100\,000$ and the number of inhibitory neurons in the network to $N_I = 10\,000$, values that correspond to 1 mm^3 of the rat cortex. The degree of connectivity is estimated to be roughly 10% [27,2]. Hence we set $f_{kl} = 0.1$ for all kl. The model neurons have two possible states 0 or 1, corresponding to a quiet state and an active one, respectively. The probability to be in each state is determined by a sigmoidal function of the local field, where the local field is equal to the total synaptic input to the neuron at a given time less the threshold, so that when equilibrium is reached

$$\tilde{S}_k^i(t) = \frac{1}{2}\{1 + \tanh[\beta(J_{kE}\tilde{S}_E(t) + J_{kI}\tilde{S}_I(t) - \theta)]\} . $$
$$(9.20)$$

Since the population average firing rates S_E, S_I are dimensionless quantities, when θ is given in mV units, the couplings should be given in mV units too, representing the total input voltage. Since in the model the couplings are equal to the total synaptic input divided by the average firing rate of the neurons in the network, the coupling constant J_{EE} can be estimated according to

$$J_{EE} = \rho_{\max}\sum_j \int V_j^{\text{EPSP}}(\tau)d\tau , \quad (9.21)$$

where V_j^{EPSP} stands for the excitatory postsynaptic potential (EPSP) induced by the jth presynaptic neuron. Similar expressions apply to the other coupling constants. Equation (9.21) represents the excitatory synaptic potential generated at the soma of an excitatory neuron if the presynaptic neurons fire (asynchronously) at their maximal rate $\rho_{\max}$. The integral over time can be ap-

proximated by the peak value of $V^{\rm EPSP}$, which is in the range of 0.1–0.5 mV, times the typical synaptic integration time, which we take to be approximately 10 msec [27]. Since one neuron receives about 5000 excitatory synapses [2], J_{EE} and J_{IE} should lie in the range of 1000–5000 mV. Although the number of inhibitory synapses is approximately 0.1 of that of the excitatory synapses, their $V^{\rm IPSP}$ is larger than $V^{\rm EPSP}$. We will therefore assume that J_{IE} is of the same order but slightly smaller than the excitatory ones, i.e., in the range of 500–2000 mV. The actual synaptic input from the excitatory population is $J_{EE}(\rho_E/\rho_{\max})$ or $J_{IE}(\rho_E/\rho_{\max})$. They fall in the range of $10-50$ mV. The synaptic input from the inhibitory population $J_{EI}(\rho_I/\rho_{\max})$ or $J_{II}(\rho_I/\rho_{\max})$ is of order 15–40 mV. For the threshold θ we choose a biologically plausible value of 20 mV, which is of the same order as the synaptic inputs. The amplitudes of the local noise $1/\beta_E$, and $1/\beta_I$, which represent fluctuations in the membrane potential, are expected to be of the same order as the threshold values, i.e., $\beta \approx 0.1$ mV^{-1}. The exact amplitude of the local noise will be determined by requiring that the model neurons maintain their low firing rates assigned above.

C. Numerical results

First we study the behavior of the network when it is far from any bifurcation point, as we expect this to be the common case. Later we will present numerical results for a network which is in the neighborhood of a bifurcation point, a Hopf bifurcation in our case.

1. Outside a bifurcation regime

For illustrating the behavior far from a bifurcation point, we choose the following set of couplings:

$$J_{EE}, \quad J_{IE}, \quad J_{EI}, \quad J_{II}$$

$$= 1230, \quad 1840, \quad -500, \quad -400 \quad \text{mV,} \quad \text{respectively} . \tag{9.22}$$

The corresponding noise amplitudes at this point are $\beta_E, \beta_I = 0.1, 0.13$ mV^{-1}, respectively. These parameters set the system in a stable fixed point. The eigenvalues of $\tilde{J}$ are $\lambda_\pm = -0.26 \pm 3i$. This eigenvalue is considerably far from any bifurcation since in general the bifurcations are characterized by eigenvalues with real part that are close to 1.

Since to leading order the equal-time ACs depend only on the average firing rates, which we keep fixed, they are, in our case, equal to $C_E(0) = \tilde{S}_E(1 - \tilde{S}_E) = 0.01$ and $C_I(0) = \tilde{S}_I(1 - \tilde{S}_I) = 0.03$ for the excitatory and inhibitory, respectively. The time-dependent ACs are shown in Fig. 4(a). They decay exponentially with the local time-constant τ_0.

The time-delayed CCs are shown in Fig. 5(a). The dominant time constant of the decay of the CCs is $0.8\tau_0$,

which is of the order as the local time constant. They oscillate in a frequency of $0.5/\tau_0$ Hz. Note that the inter-population CCs are not symmetrical because the populations are coupled with each other via asymmetric couplings: $J_{IE} \geq 0$, while $J_{EI} \leq 0$. In fact, there is an average delay between the activities of the two populations which equals $0.3\tau_0$ and the ratio between the peak value and $C_{EI}(0)$ is 1.6. The amplitude of the CCs can be judged by their value at equal times, which are $0.07/N$, $0.13/N$, and $0.2/N$ for $C_{EE}(0)$, $C_{IE}(0)$, and $C_{II}(0)$, respectively. A useful way to normalize these amplitudes is to consider

$$\frac{C_{kl}(0)}{\sqrt{C_k(0)C_l(0)}} , \tag{9.23}$$

which are the *correlation coefficients* of the variables S_k and S_l. In the present case these coefficients are $\approx 7/N$, in agreement with the general expectation.
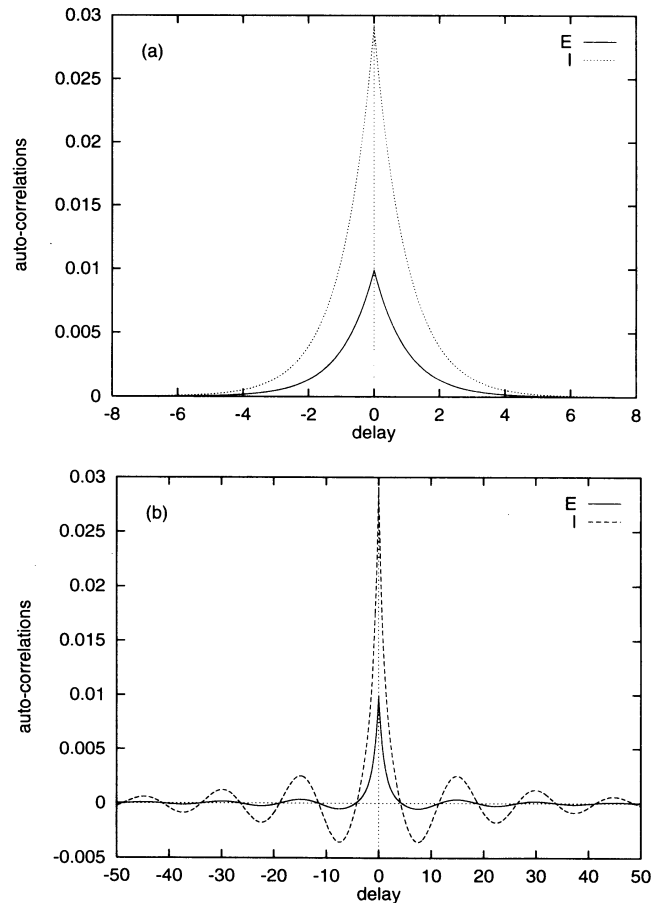
The above results correspond to the population aver-

FIG. 4. Population-averaged time-delayed autocorrelations of excitatory (E) and inhibitory (I) neurons. (a) Interaction parameters are the same as in Eq. (9.22), which is outside the bifurcation regime; see text. (b) Parameters are the same as in Eq. (9.25) with bifurcation parameter $\alpha = 0.05$, which is close to the bifurcation point. Note the change in the scale of time.

aged CCs. However, due to inhomogeneity of the network, the CCs between individual pairs of neurons show additional features. In Fig. 6(a) we present $C^{ij}_{EE}(\tau)$ for three types of pairs as described in details in Sec. VIII. As can be seen, the CC between reciprocally connected pairs is about four times larger than the average. This case is,
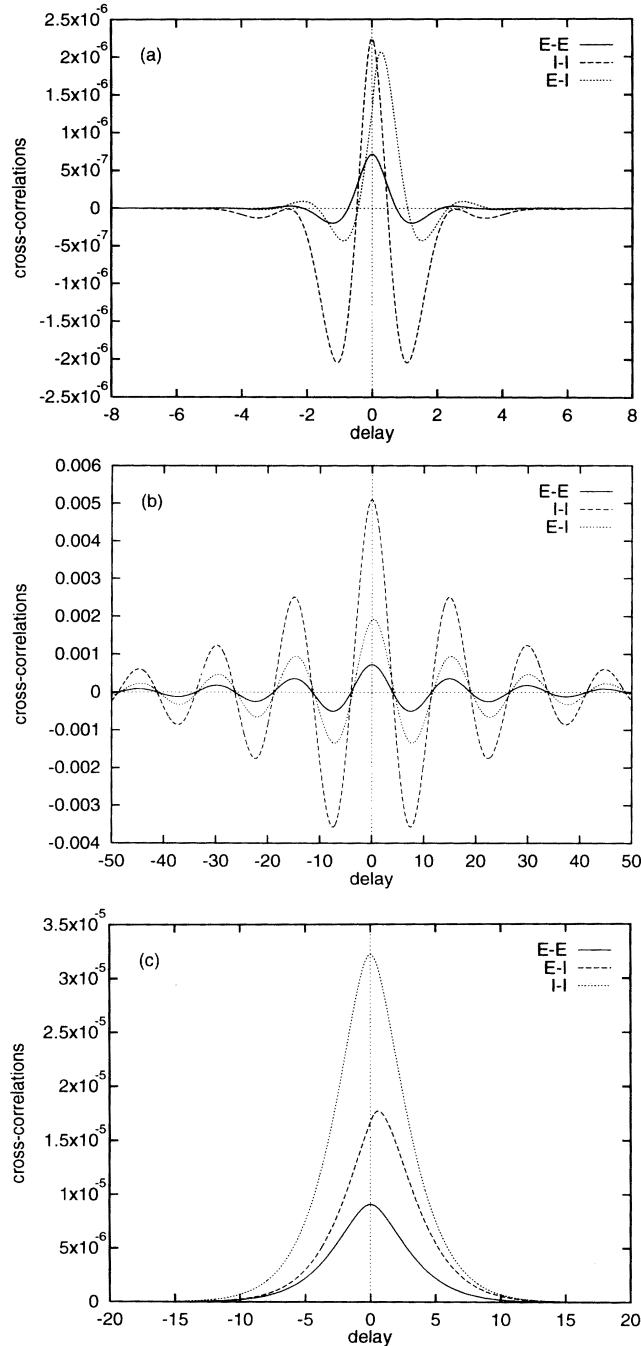
however, extremely rare. There is also an increase by a factor larger than 2 in the magnitude of the CC of pairs connected unidirectionally (i.e., $\bar{J}^{ji}_{EE} > 0$ while $\bar{J}^{ij}_{EE} = 0$), relative to the average value. Moreover, $C_{EE}(\tau)$ exhibits a delay (of $0.15\tau_0$) in the peak value, accompanied by a prominent shoulder at about $2\tau_0$. Both the increase in the magnitude and the asymmetric shape of the CC are indicative of the important contribution of the direct coupling to the correlation between the fluctuations of this pair. This is indeed expected. The CCs between directly coupled neurons scale as $1/(fN)$, while the average CCs scale only as $1/N$. This difference is large in the case of a strong dilution, such as ours where $f = 0.1$. In other words, in the case of a strong dilution, the total synaptic input of a neuron consists of relatively few synaptic events; hence each synapse is relatively strong. Finally, the correlation between neurons with no direct interaction is smaller than the average by about 30%.
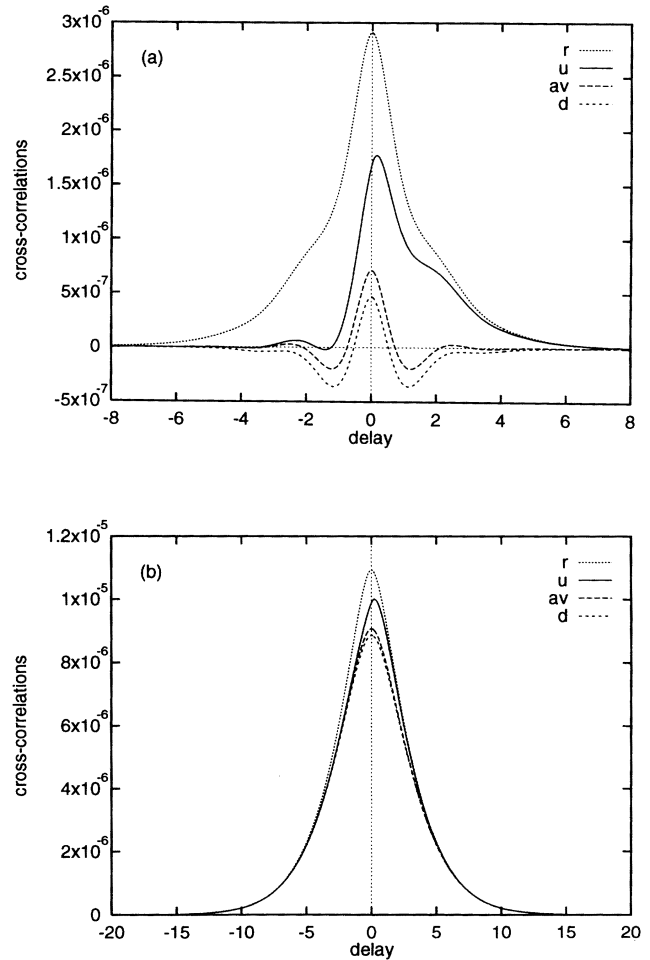

FIG. 5. Population-averaged time-delayed cross correlations between excitatory-excitatory (E-E), inhibitory-inhibitory (I-I), and excitatory-inhibitory (E-I) pairs. (a) Outside the bifurcation regime. (b) Close to the bifurcation point $\alpha=0.05$. (c) In the bifurcation regime $\alpha = 0.5$. Note the change in scales of time.

FIG. 6. Time-delayed cross correlations between excitatory-excitatory pairs in a randomly dilute network. Reciprocally connected (r), unidirectionally connected (u), and disconnected (d) pairs are shown. For comparison we present again the population-averaged results (av). (a) Outside the bifurcation regime. (b) In the bifurcation regime ($\alpha=0.5$).

2. The bifurcation regime

We present numerical solutions of the equations for the correlation functions for parameters which are in the neighborhood of the Hopf bifurcation which occurs at

$$J^0_{EE}, \quad J^0_{IE}, \quad J^0_{EI}, \quad J^0_{II}$$

$$= 1730, \ 1540, \ -500, \ -400 \ \text{mV} \ , \ \text{respectively} \ .$$
(9.24)

The noise amplitudes at the bifurcation are $\beta_E, \beta_I = 0.13, 0.10 \ \text{mV}^{-1}$, respectively. All other parameters are set to values that were previously presented. We vary the values of the couplings by choosing them to be equal to the bifurcation point up to an overall constant, i.e.,

$$J_{kl} = (1 - \alpha)J^0_{kl} \ , \quad \alpha < 1 \ .$$
(9.25)

The parameter α indicates the proximity to the bifurcation point and can be called the control parameter of our system. When $\alpha = 0$ the system is at the bifurcation point, whereas $0 < \alpha < 1$ corresponds to the regime where the system has a stable fixed point (with low firing rates). The range $\alpha < 0$ corresponds to the regime where the low rate fixed point becomes unstable.

The Hopf bifurcation at Eq. (9.24) is a supercritical Hopf bifurcation [22], meaning that the stable fixed point is surrounded by an unstable limit cycle that collapses onto the fixed point as α decreases to 0. This is shown in Fig. 7, where we plot the unstable limit cycle that surrounds the fixed point, for $\alpha = 0.05$ and 0.03. As we approach the bifurcation point, the network is expected to demonstrate a critical behavior in which the leading term in the equal-time CCs is much larger than $1/N$ and can be even of order 1, as discussed earlier [Eq. (7.3)], and the dominant decay constant diverges. This is shown in Fig. 8, where the equal-time CCs and the largest time constant are plotted as functions of α. These results are reliable only for α not too close to 0. When the system is very close to the bifurcation, the theory by which the CCs are computed is inapplicable since it relied on the smallness of the fluctuations in the synaptic fields.

We illustrate the behavior close to the bifurcation point by taking $\alpha = 0.05$, i.e., J_{EE}, J_{EI}, J_{IE}, and $J_{II} = 1644, 1463, 475$, and 380 mV, respectively. The corresponding noise amplitudes are $\beta_E, \beta_I = 0.13, 0.11 \ \text{mV}^{-1}$, respectively. In this case, $\lambda_{\pm} = 0.95 \pm 1.4i$. In Fig. 4(b), we present the time-delayed ACs $C_E(\tau)$ and $C_I(\tau)$ as functions of the delay. In this figure we have incorporated the $O(1/N)$ corrections, Eq. (6.22). As can be seen, near the bifurcation and for the values of N_E and N_I that we have chosen above, the cooperative contributions to the ACs are no longer small and give rise to a pronounced damped oscillations in the ACs. The time-delayed CCs are shown in Fig. 5(b). Their value at zero delay, the equal-time CCs, is much larger than $1/N \approx 10^{-5}$. The time-delayed CCs decay with time constant of $20\tau_0$, oscillating with frequency of $0.22/\tau_0$. Note that the ratio of the peak to the zero-delay value of C_{EI} is close to 1.

This is because near the bifurcation the CC is dominated by the critical mode, which, in this case, peaks at zero delay.

Our last numerical example corresponds to the case where the system is further away from the bifurcation, but is still affected by it. This is the case of $\alpha = 0.5$. The local noises β_E and β_I are computed to be 0.12 and 0.09 mV^{-1}, respectively. In this case, $\lambda_{\pm} = 0.49 \pm 0.65i$. The ACs decay exponentially, similarly to the case of Fig. 4(a). The time-delayed CCs for this case are shown in Fig. 7(c). The correlation coefficients are $\approx 70/N$, indicating that the system is still affected by the bifurcation point. On the other hand, the dominant time constant of the decay of the CCs is small $\approx 2.0\tau_0$. The frequency of the damped oscillations is $0.1/\tau_0$ Hz. Note that although the frequency is not a critical quantity, it is affected by the increase in α, as a comparison with the case of $\alpha = 0.05$ reveals. The decrease in the frequency is due to the fact that decreasing the couplings simultane-
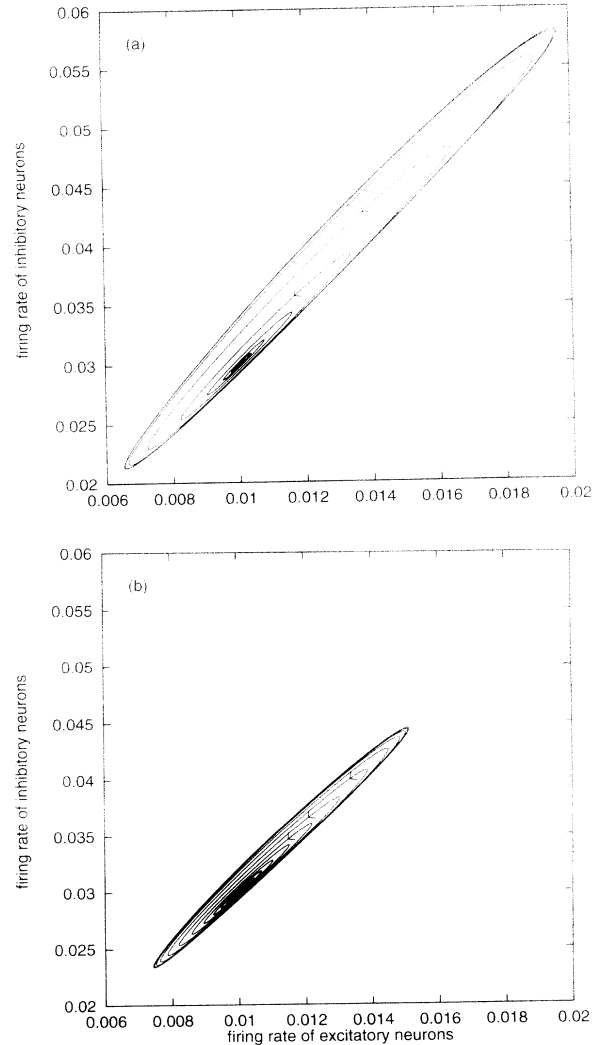

FIG. 7. Unstable limit cycle around the stable fixed point for network parameters Eq. (9.25) for two values of α: (a) $\alpha = 0.05$ and (b) $\alpha = 0.03$.

ously implies a decrease of the imaginary part of $\lambda_\pm$ by a similar factor $(1 - \alpha)$ as long as the local noise does not change significantly. The average delay between the activities of the two populations equals $0.6\tau_0$ and the ratio between the peak value and $C_{EI}(0)$ is 1.06. In Fig. 6(b) we present $C_{EE}^{ij}(\tau)$ for the individual pairs. The effects of inhomogeneity are significant, but are less prominent than in the case where the system was far from a bifurcation. This is due to the fact that the net addition of inhomogeneity is almost unchanged, while the size of the average CCs is now one magnitude larger. In the reciprocal case the CCs peak value is 1.2 times the peak value of the averaged CCs. In the unidirectional case, the addition to $C_{EE}(0)$ is such that $C_{EE}^{ij}(0)/C_{EE}(0) = 1.3$ and $C_{EE}(\tau)$ exhibits a delay of $0.22\tau_0$ in the peak value, with a peak to zero-delay ratio of 1.05. In the disconnected case, the correlations are slightly smaller than the average, where the maximal decrease in the correlations, which is obtained at zero delay, is 2% of the peak value of the averaged cross correlations.
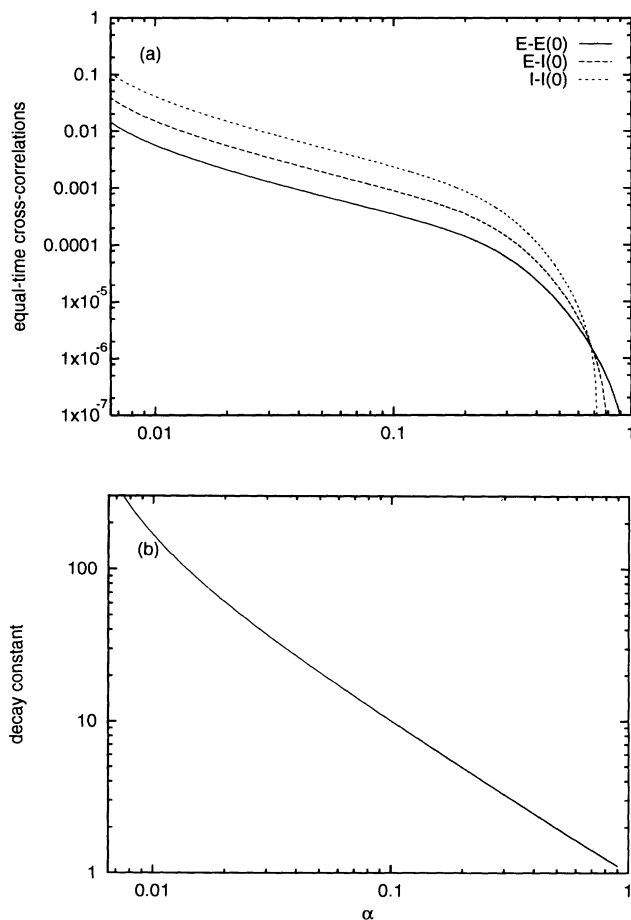

FIG. 8. Critical behavior of the cross correlations near a bifurcation. (a) Equal-time cross correlations of population-averaged excitatory-excitatory $[E - E(0)]$, inhibitory-inhibitory $[I - I(0)]$, and excitatory-inhibitory $[E - I(0)]$ pairs as a function of α. (b) Dependence of the largest time constant on α.

X. DISCUSSION

We have presented a theory of the correlation functions and linear response in large stochastic networks with high degree of connectivity. Our theory is an extension of the mean-field theory of the kinetic Ising models near thermal equilibrium [21,20,28]. The systems studied here do not obey the detailed-balance conditions; hence their statistics are not described by thermal equilibrium. In order for detailed balance to hold the connections must be symmetric $J^{ij} = J^{ji}$ and there are constraints on the form of the transfer function in the transition rates Eq. (3.1) [20,28]. These conditions result in a significant simplification of the theory. The fundamental eigenmodes of the fluctuations are orthogonal and their eigenvalues are real. Thus the resultant time dependence of the correlation and response functions is relatively simple, as they are composed of a sum of pure, exponentially decaying orthogonal modes. In addition, systems with detailed balance obey the fluctuation dissipation theorem [29], which establishes a direct relationship between the time-dependent response and the correlations.

In contrast, in the present work, symmetry of the connection matrix has not been assumed, nor have we restricted the detailed form of the sigmoidal transfer function. As a result, the fundamental modes of the response and fluctuations are not orthogonal and their eigenvalues are in general complex. Also, there is no simple relationship between response and fluctuations. These factors significantly complicate the theoretical calculations as well as the identification of the modes from measurements. In addition, the resultant time dependence is richer and may include in general damped oscillatory modes. Furthermore, although each mode is decaying exponentially at all times the response to certain small perturbations may initially grow in time. This phenomenon may lead to a substantial transient amplification of certain perturbations, although at long times the total response will decay exponentially [30]. Such a behavior cannot occur if the eigenmodes are orthogonal, as is the case with systems at thermodynamic equilibrium.

Despite these differences, there are some important similarities between the equilibrium case and the more general case considered here. Even in the absence of detailed balance, the response and the correlations are governed by the same fundamental modes. In both cases, these modes are directly related to the interactions through the effective interaction matrix Eq. (4.5). One of the main results of the present work is the critical behavior at a bifurcation point, which has been discussed in Sec. VIII. This behavior is similar in many respects to the mean-field phase transition that occurs in analogous systems at thermal equilibrium.

The results of the present theory can be applied to study the correlations in a variety of biologically interesting network models. A simple example is the case of excitatory-inhibitory network studied in Sec. IX. This architecture is commonly used in modeling local neuronal circuits in the brain. Our theory can be used to calculate the neuronal correlations in recurrent, associative-memory networks modeling hippocampal [31] or extra-

striatal visual areas [32]. Provided that the number of embedded memories is far below the capacity [33], these networks have a connectivity patterns that falls within the framework of this work. Another potential area of application is in the study of sensory or motor cortical systems, where the gross organization of the intrinsic connections is known.

Is the predicted critical behavior of the correlations and response functions at a bifurcation point relevant to biological systems? In general, one has to fine-tune the parameters of the system to bring it close to a bifurcation point. Such a fine-tuning may seem unlikely in many realistic situations. However, there are interesting cases where symmetry considerations dictate that the system is near a bifurcation point. Examples are systems that code for orientation or direction of sensory or motor signals [34]. In addition, in some cases operating near a bifurcation point may be functionally important, such as in the case of olfaction [6] or the vestibuocular system [35]. A learning mechanism may be responsible for maintaining these systems near the bifurcation point [35,36]. The above theory can then be used to predict the behavior of the dominant mode of fluctuations.

To apply the theory to realistic situations, several extensions have to be made. First, one has to consider inhomogeneity in the local parameters, e.g., the local thresholds or time constants. This type of inhomogeneity is more difficult to treat than random inhomogeneity in the interactions, studied in Sec. VIII. In addition, it is important to consider a more general dynamic model, which will incorporate refractoriness as well as synaptic delays. Although dynamics with delays is non-Markovian, it may still be possible to study the correlations in networks with mean-field architecture.

The present theory is limited to asynchronous states in networks with a high degree of connectivity. The assumption of high connectivity is realistic in many brain structures, and although the probability of connections may fall off with distance, such a dependence may be incorporated within our framework. However, the biological plausibility of the assumption asynchronicity of the dynamic state is questionable. In fact, our theory may provide means of testing this assumption. The asynchronous states are characterized by CCs with amplitudes of the order of $1/N$ and by the fact that the contribution to the CCs of a pair of neurons from the direct connections between them is in general of the same order of magnitude as the total CCs. In contrast, synchronous states are characterized by CCs which are of order 1 even if the system is a large, fully connected network, so that the contribution from a given direct connection is still of order $1/N$. This implies that in synchronous states, the CCs are dominated by the coherent dynamics of the system and will be much less sensitive to the value of the direct connection between a given pair.

Unfortunately, comparison with experimental data is complicated by the need to find an appropriate normalization of cross correlograms of experimentally measured spike trains. This issue is discussed in detail elsewhere [37]. However, insight may be gained by analyzing the observed temporal behavior of the correlation functions.

For instance, according to our theory, the ACs are dominated by the local noise, whereas the CCs are strongly affected by the cooperative fluctuations which may have relatively long decay times. Thus comparing the time dependence of the ACs and the CCs may give an important clue on this issue. In addition, it may be possible to measure the effect of perturbing the synaptic connections between a pair of neurons on their CCs within the network. Finally, although we have focused here only on asynchronous states, analytic calculation of the correlation functions in certain synchronous states may be possible. An example is the case of stochastic phase oscillators studied in Refs. [9,10]. Thus generalizing the present approach to calculate the correlation functions of weakly synchronized states in systems with mean-field architecture is an important challenge for future research.

ACKNOWLEDGMENTS

APPENDIX A

In this appendix we derive the equations for averages and correlation functions for a general network with the stochastic dynamics defined in Sec. III. In this appendix we do not assume any specific connection architecture and will therefore use the notation where subscripts denote neuronal indices. Our derivation is similar to that given in Ref. [21] for an Ising system with transition rates that obey detailed balance.

The equation for the average activities is given by

$$\frac{d}{dt}\langle S_i(t)\rangle = \sum_{\{S\}} S_i \frac{d}{dt} P(\{S\}, t) , \qquad (A1)$$

where $\sum_{\{S\}}$ represents summation over all possible configurations $\{S\} = (S_1, \ldots, S_N)$. Substituting Eq. (3.3) into Eq. (A1) yields:

$$\frac{d}{dt}\langle S_i(t)\rangle = -\sum_{\{S\}} \sum_{l=1}^{N} S_i w(S_l) P(\{S\}, t)$$

$$+ \sum_{\{S\}} \sum_{l=1}^{N} S_i w(1 - S_l) P(\{S\}^l, t) , \qquad (A2)$$

where $w(S_l)$ stands for $w(S_l \to (1-S_l))$, $w(1-S_l)$ stands for $w((1-S_l) \to S_l)$, and $\{S\}^l \equiv (S_1, \ldots, 1-S_l, \ldots, S_N)$. Since the above summations are over all possible configurations, each configuration in which $S_l = 1$ has

a complementary configuration in which $S_l = 0$ and vice versa. We can therefore replace the expressions $S_i w(1 - S_l) P(\{S\}^l)$ by $S_i w(S_l) P(\{S\})$ for $i \neq l$ and $S_i w(1 - S_i) P(\{S\}^i)$ by $(1 - S_i) w(S_i) P(\{S\})$. We thus rewrite Eq. (A2) as

$$\frac{d}{dt} \langle S_i(t) \rangle = \sum_{\{S\}} \left[- \sum_{l=1}^{N} S_i w(S_l) + \sum_{\substack{l=1 \\ l \neq i}}^{N} S_i w(S_l) \right.$$

$$\left. + (1 - S_i) w(S_i) \right] P(\{S\}, t) . \qquad (A3)$$

The terms in the first summation, for which $l \neq i$, are canceled by the corresponding terms in the second summation and we are left with

$$\frac{d}{dt} \langle S_i(t) \rangle = \sum_{\{S\}} (1 - 2S_i) w(S_i) P(\{S\}, t) , \qquad (A4)$$

which is equivalent to

$$\frac{d}{dt} \langle S_i(t) \rangle = \langle (1 - 2S_i) w(S_i) \rangle . \qquad (A5)$$

Here and in the following, the angular brackets stand for an averaging with respect to P at time t. Using the form of the transition probabilities Eq. (3.1) and the fact that $S_i = 0, 1$, one obtains the result of Eq. (3.4). A similar derivation yields, for the second-order moments,

$$\tau_0 \frac{d}{dt} \langle S_i(t) S_j(t) \rangle = -2 \langle S_i S_j \rangle + \langle S_i g(h_j) \rangle + \langle S_j g(h_i) \rangle . \qquad (A6)$$

Using Eq. (A5) we obtain the result of Eq. (3.6) for the equal-time correlation functions.

So far, we have evaluated quantities that depend on a single time t. To calculate time-delayed correlations we have to average quantities that depend on two different times t and $t + \tau$, $\tau > 0$. This is done by averaging over t, weighted by the initial probabilities $P(\{S\}, t)$, and over configurations at the later time $t + \tau$, weighted by the conditional probabilities $P(\{\sigma\}, t + \tau | \{S\}, t)$. This quantity is the probability of finding the system at state $\{\sigma\}$ at time $t+\tau$, given that it was in the state $\{S\}$ at time t. The equations for the "two-time" second moments are then

$$\frac{d}{d\tau} \langle S_i(t) S_j(t + \tau) \rangle$$

$$= \sum_{\{S\}} \sum_{\{\sigma\}} S_i \sigma_j \frac{d}{d\tau} P(\{\sigma\}, t + \tau | \{S\}, t)$$

$$\times P(\{S\}, t), \quad \tau > 0 . \qquad (A7)$$

The conditional probabilities obey the same master equation as in Eq. (3.3). Using Eq. (A1), we obtain

$$\tau_0 \frac{d}{d\tau} \langle S_i(t) S_j(t + \tau) \rangle = - \langle S_i(t) S_j(t + \tau) \rangle$$

$$+ \langle S_i(t) g(h_j(t + \tau)) \rangle ,$$

$$\tau \geq 0 . \quad (A8)$$

A similar derivation for a system at thermal equilibrium is presented in [21]. Using Eqs. (A8) and (3.4) one obtains the result of Eq. (3.7).

APPENDIX B

In this appendix we derive approximations of the results of Appendix A which are exact for highly connected networks in the limit of large networks. Specifically, we will assume that each neuron is connected to a number of neurons of order N with connections J_{ij} that are all of order $1/N$. Implicitly, we assume that the large N limit is well defined by keeping the population architecture specified in Sec. II. However, we will use the general notation of Appendix A, denoting by subscripts neuronal indices, and will not explicitly refer to population indices.

First we consider Eq. (3.4) for the average activities. We write

$$h_i = \langle h_i \rangle + \delta h_i , \qquad (B1)$$

where $\langle h_i \rangle = \sum_j J_{ij} \langle S_j \rangle$ and $\delta h_i = \sum_j J_{ij} \delta S_j$. We then obtain

$$\langle g(h_i) \rangle \approx g(\langle h_i \rangle) + \frac{1}{2} g''(\langle h_i \rangle) \sum_{jk} J_{ij} J_{ik} C_{jk}(0) . \qquad (B2)$$

Taking into account that C_{jk} are of order $1/N$ for all $j \neq k$ and the strength of the connections it is readily seen that the last term is of order $1/N$. Hence, to leading order one obtains, for the dynamics of the average activities,

$$\tau_0 \frac{d}{dt} \langle S_i(t) \rangle = - \langle S_i \rangle + g(\langle h_i \rangle) \qquad (B3)$$

and

$$\langle S_i \rangle = g(\langle h_i \rangle) , \qquad (B4)$$

which corresponds to Eqs. (4.1) and (4.2).

To approximate the CCs, we expand the quantities

$$\langle \delta S_i(t) g(h_j(t + \tau)) \rangle = \langle \delta S_i(t) \delta g(h_j(t + \tau)) \rangle \qquad (B5)$$

in powers of δh_j. The leading order contribution to Eq. (B5) is

$$\langle \delta S_i(t) \delta g_j(t + \tau) \rangle \approx \sum_k \tilde{J}_{jk}(t + \tau) C_{ik}(t, t + \tau) , \qquad (B6)$$

where $\tilde{J}_{ij}(t) \equiv g'(\langle h_i(t) \rangle) J_{ij}$. Each of the terms with $k \neq i$ are of order $1/N^2$. The term with $k = i$ involves the ACs and is therefore of order $1/N$. The total contribution from both sources is of order $1/N$. Thus Eq. (3.6) reduces to

$$\tau_0 \frac{d}{dt} C_{ij}(t, t) = - 2 \langle \delta S_i \delta S_j \rangle + \langle \delta S_i g(h_j) \rangle$$

$$+ \langle \delta S_j g(h_i) \rangle . \qquad (B7)$$

Equation (3.9) for the equal-time CCs at equilibrium reduces to

$$2C_{ij}(0) = \sum_{k=1}^{N} \tilde{J}_{jk}C_{ik}(0) + \sum_{k=1}^{N} \tilde{J}_{ik}C_{jk}(0)$$
$$+ \tilde{J}_{ji}C_{ii}(0) + \tilde{J}_{ij}C_{jj}(0) \ , \quad i \neq j \ . \qquad (B8)$$

Similarly, the equation for the equilibrium time-delayed CCs reduces to

$$\tau_0 \frac{d}{d\tau}C_{ij}(\tau) = -C_{ij}(\tau) + \sum_{k=1}^{N} \tilde{J}_{jk}C_{ik}(\tau) + \tilde{J}_{ji}C_{ii}(\tau) \ ,$$

$$i \neq j \ . \quad (B9)$$

Equations (B8) and (B9) are equivalent to the matrix equations (6.8) and (6.15). A similar derivation holds for the $1/N$ corrections to the time-delayed autocorrelations Eq. (6.22).

APPENDIX C

In this appendix we provide the full solution of the CCs in the two-population network described in Sec. VI. The three equal-time CCs $C_{EE}(0)$, $C_{II}(0)$, and $C_{EI}(0) = C_{IE}(0)$ obey Eq. (6.14) with $C_{\mu\nu}$, $\nu, \mu, = \pm$ defined in Eq. (6.10). In our case, the eigenvalues and eigenvectors are given in Eqs. (9.9)–(9.11). The matrix $C_{\mu\nu}$ equals

$$C_{\mu\nu} = \frac{c_\mu c_\nu (\lambda_\mu + \lambda_\nu)}{(2 - \lambda_\mu - \lambda_\nu)}[\tilde{J}_{IE}^2 N_E^{-1}C_E(0)$$
$$+ (\lambda_\mu - \tilde{J}_{EE})(\lambda_\nu - \tilde{J}_{EE})N_I^{-1}C_I(0)] \ , \qquad (C1)$$

where

$$c_\mu = [\tilde{J}_{IE}\tilde{J}_{EI} + (\lambda_\mu - \tilde{J}_{EE})^2]^{-1/2} \qquad (C2)$$

and C_E and C_I are the ACs of the two populations. Note that $C_{\mu\nu}$ is symmetric with respect to μ and ν. From these expressions it is clear that the CCs will diverge whenever the denominator of $C_{\mu\nu}$ gets close to zero. When a saddle-node bifurcation is approached, $\lambda_\pm$ are both real and C_{++} will diverge while other $C_{\mu\nu}$ will remain finite. When a Hopf bifurcation is approached, $\lambda_\pm$ are complex and C_{+-} and C_{-+} will diverge. At both bifurcations all equal-time CCs will diverge since they all depend on all the terms of $C_{\mu\nu}$.

Using the general equation derived for the time-delayed CCs [Eq. (6.20)], we find the time-dependent CCs, for the two populations network Eq. [(9.17)], where the coefficients $a_{kl}^{\pm}$ are given by

$$a_{kl}^{+} = C_{k1}(0)L_1^{+} + C_{k2}(0)L_2^{+} + \frac{C_k(0)}{N_k}\lambda_+ L_k^{+} \ .$$
$$a_{kl}^{-} = C_{k1}(0)L_1^{-} + C_{k2}(0)L_2^{-} + \frac{C_k(0)}{N_k}\lambda_- L_k^{-} \ , \qquad (C3)$$
$$a_{kl}^{0} = \delta_{kl}N_k^{-1}C_k(0) \ .$$

[1] E. Fetz, K. Toyama, and W. Smith, in *Cerebral Cortex*, edited by A. Peters and G. Jones (Plenum Press, New York, 1991), Vol. 9.

[2] M. Abeles, *Corticonics: Neural Circuits of the Cerebral Cortex* (Cambridge University Press, Cambridge, 1991).

[3] K. H. Britten, M. N. Shadlen, W. T. Newsome, and J. A. Movshon, J. Neurosci. **12**, 4745 (1992).

[4] H. S. Seung and H. Sompolinsky (unpublished).

[5] C. A. Skarda and W. J. Freeman, Behav. Brain Sci. **10**, 161 (1987).

[6] Z. Li and J. J. Hopfield, Biol. Cybern. **61**, 379 (1989).

[7] C. M. Gray, P. Konig, A. K. Engel, and W. Singer, Nature (London) **338**, 334 (1989).

[8] R. Eckhorn et al., Biol. Cybern. **60**, 121 (1988).

[9] H. Sompolinsky, D. Golomb, and D. Kleinfeld, Proc. Natl. Acad. Sci. U.S.A. **87**, 7200 (1990); Phys. Rev. A **43**, 6990 (1991).

[10] E. Grannan D. Kleinfeld, and H. Sompolinsky, Neural Comput. **4**, 550 (1992).

[11] M. Abeles, H. Bergman, E. Margalit, and E. Vaadia, J. Neurophysiol. **70**, (1993).

[12] E. Ahissar, E. Vaadia, M. Ahissar, H. Bergman, A. Arieli, and M. Abeles, Science **257**, 1412 (1992).

[13] I. Ginzburg and H. Sompolinsky, in *Advances in Neural Information Processing Systems*, edited by J. D. Cowan, G. Tesauro, and J. Alspector (Morgan Kaufmann, San Mateo, CA, 1994), Vol. 6.

[14] S. Kirkpatrick and D. Sherrington, Phys. Rev. B **17**, 4384 (1978).

[15] D. J. Amit, H. Gutfreund, and H. Sompolinsky, Ann. Phys. (N.Y.) **173**, 30 (1987).

[16] T. Bohr, G. Grinstein, Y. He, and C. Jayaprakash, Phys. Rev. Lett. **58**, 2155 (1987).

[17] I. Aranson, D. Golomb, and H. Sompolinsky, Phys. Rev. Lett. **68**, 3495 (1992).

[18] D. Hansel and H. Sompolinsky, Phys. Rev. Lett. **68**, 718 (1992), and (unpublished).

[19] N. G. Van Kampen, *Stochastic Processes in Physics and Chemistry* (North-Holland, Amsterdam, 1981).

[20] R.J. Glauber, J. Math. Phys. **4**, 294 (1963).

[21] M. Suzuki and R. Kubo, J. Phys. Soc. Jpn. **24**, 51 (1968).

[22] J. Guckenheimer and P. Holmes, *Nonlinear Oscillations, Dynamic Systems, and Bifurcations of Vector Fields* (Springer, New York, 1983).

[23] K. Binder and D. N. Heerman, *Monte Carlo Simulation in Statistical Physics* (Springer-Verlag, Berlin, 1988).

[24] H. Sompolinsky (unpublished).

[25] H. R. Wilson and J. D. Cowan, Biophys. J. **12**, 1 (1972).

[26] H. G. Schuster and P. Wagner, Biol. Cybern. **64**, 77 (1990).

[27] A. Mason, A. Nicoll, and K. Stratford, J. Neurosci. **11**, 72 (1991).

[28] K. Kawasaki, in *Phase Transitions and Critical Phenomena*, edited by C. Domb and M. S. Green (Academic Press, New York, 1972), Vol. 2.

[29] S.-K. Ma, *Modern Theory of Critical Phenomena* (Benjamin, Reading, MA, 1976).

[30] L. N. Trefethen, A. E. Trefethen, S. C. Reddy, and T. A. Driscoll, Science **261**, 587 (1993).

[31] B. L. McNaughton and R. G. M. Morris, Trends Neurosci. **10**, 408 (1987).

[32] M. Griniasty, M. Tsodyks, and D. J. Amit, Neural Com-

put. **5**, 1 (1993).

[33] D. J. Amit, H. Gutfreund, and H. Sompolinsky, Phys. Rev. A **32**, 1007 (1985).

[34] R. Ben-Yishai, R. Lev Bar-Or, and H. Sompolinsky (unpublished).

[35] S. C. Cannon , D. A. Robinson, and S. Shamma, Biol. Cybern. **49**, 127 (1983).

[36] D. Lehmann and E. Binenstock, private communication.

[37] M. Abeles, I. Ginzburg, and H. Sompolinsky (unpublished).